Advancements in the Development of non-BET Bromodomain Chemical Probes

Michael A. Clegg[a],[b], Nicholas C. O. Tomkinson[b], Rab K. Prinjha[a] and Philip G. Humphreys*[a]

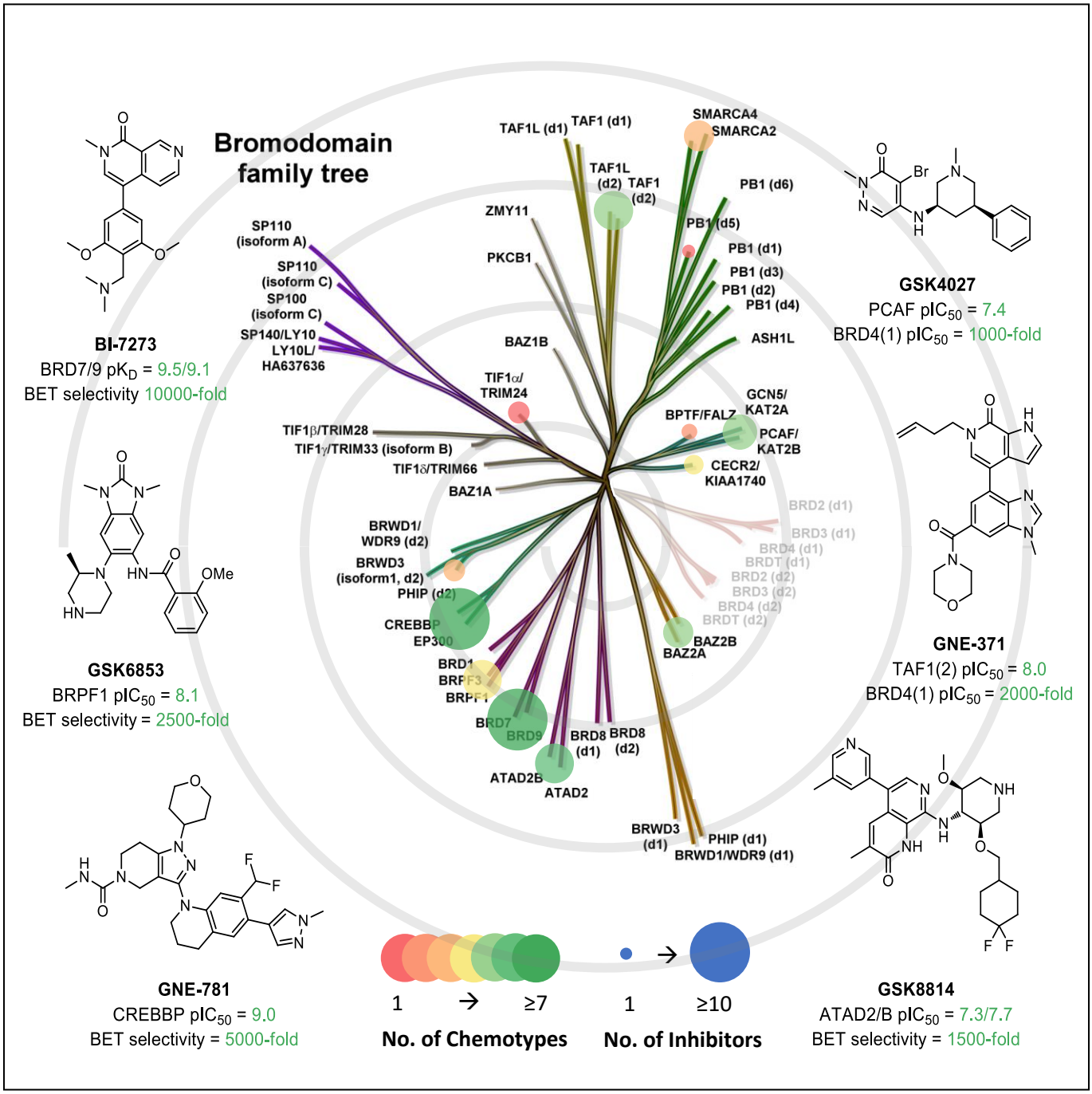

BI-7273
BRD7/9 pK_D = 9.5/9.1
BET selectivity 10000-fold

GSK4027
PCAF pIC_{50} = 7.4
BRD4(1) pIC_{50} = 1000-fold

GSK6853
BRPF1 pIC_{50} = 8.1
BET selectivity = 2500-fold

GNE-371
TAF1(2) pIC_{50} = 8.0
BRD4(1) pIC_{50} = 2000-fold

GNE-781
CREBBP pIC_{50} = 9.0
BET selectivity = 5000-fold

GSK8814
ATAD2/B pIC_{50} = 7.3/7.7
BET selectivity = 1500-fold

Abstract: The bromodomain and extra terminal (BET) family of bromodomain containing proteins (BCPs) have been the subject of extensive research over the past decade, resulting in a plethora of high quality chemical probes for their tandem bromodomains. In turn, these chemical probes have helped reveal the profound biological role of the BET bromodomains and their role in disease, ultimately leading to a number of molecules in active clinical development. However, the BET subfamily represents just 8/61 of the known human bromodomains, and attention has now expanded to the biological role of the remaining 53 non-BET bromodomains. Rapid growth of this research area has been accompanied by a greater understanding of the requirements for an effective chemical probe and has led to a number of new non-BET bromodomain chemical probes being developed. Recent efforts since December 2015 will be discussed here, highlighting the particular strengths/caveats of each molecule, and the value they add in validating an untapped source of therapeutics.

1. Introduction

Epigenetics is defined as the study of heritable changes in gene expression without alteration of the underlying DNA sequence.[1] Instead, epigenetic modifications operate by disrupting the structure of chromatin and thus modulating the accessibility of DNA. One of the most extensively studied and well recognised modifications is the acetylation of lysine residues present on histone tails,[2–4] a process regulated by histone acetyltransferases (HATs) and histone deacetyltransferases (HDACs), which 'write' and 'erase' acetyl marks respectively.

Acetylated lysine (KAc) residues are recognised by 'reader' modules known as bromodomains which selectively bind to context sensitive acetylated lysine residues, recruiting cellular transcriptional machinery to a specific histone mark, and regulating gene expression. The structure of bromodomains is comprised of a unique left-handed bundle consisting of four antiparallel alpha helices (αZ, αA, αB, and αC) connected by two flexible loop regions (ZA and BC), which together form the hydrophobic pocket for acetylated lysine binding (**Figure 1**).[5] Within the binding pocket of typical human bromodomains (48/61) are two conserved amino acid residues (Asn and Tyr) which together form the two key interactions for acetylated lysine recognition. More specifically, a direct hydrogen bond is formed between the KAc carbonyl moiety and the NH_2 of the conserved Asn residue, whilst a water mediated hydrogen bond interaction is formed to the hydroxy group of the conserved Tyr. The size of the KAc binding pocket and the conserved H-bonding interactions has led to substantial success in the development of small molecule typical bromodomain inhibitors, designed to competitively mimic these interactions. By contrast, in 13/61 of human bromodomains, the conserved Asn residue is mutated to either a Tyr, Thr or Asp. These are known as 'atypical' bromodomains and have proven more difficult to design competitive inhibitors for in the past.

Despite a good understanding of bromodomain function and structure, the biological role of BCPs in modulating healthy and disease states is still unclear. As a result, there is a need for high quality chemical probes to be used as part of pre-clinical target validation to help elucidate the biological functions of these proteins, and specifically, whether the bromodomain regions themselves play an active role.

A chemical probe is a tool molecule that selectively binds to a target and is used to elucidate its biological function,[6,7] helping bridge together chemical biology and drug discovery. In contrast to other target validation methods, such as gene knockdown, in which the actions of the entire complex is blocked, chemical probes allow for elucidation of the biological roles of each individual domain, making them particularly attractive for bromodomain target validation.

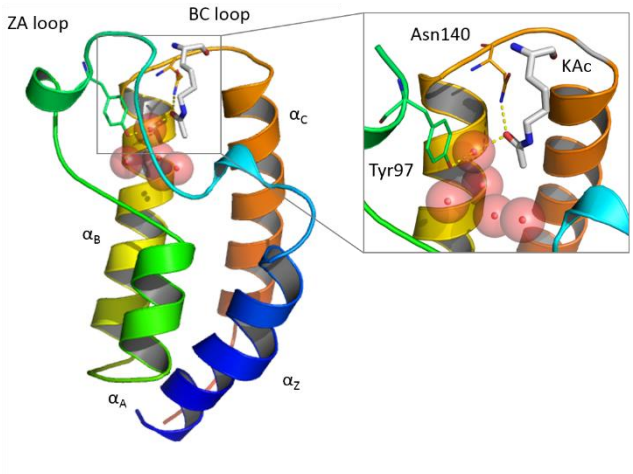

Figure 1. X-ray crystal structure of BRD4(1), highlighting the four antiparallel alpha helices, loop regions, and the key interactions formed between typical bromodomains and acetylated lysines.

The necessity for high quality probes has been highlighted in a number of excellent reviews[8–10], with clear guidelines defined for probe generation. This, combined with bodies such as the SGC, Chemical Probes Portal and the Open Science Probe Project, aimed at increasing the quality, availability and reproducibility of research using chemical probes, has led to an important and necessary improvement to the quality and supporting data accompanying molecules being proposed as chemical probes. To summarise Bunnage and co-workers[11], for effective target validation a chemical probe must: 1) be able to reach the site of action at pharmacologically relevant concentrations; 2) display in vitro evidence of target engagement

[a] M. A. Clegg, Dr. R. K. Prinjha, Dr. P. G. Humphreys
Epigenetics Discovery Performance Unit
GlaxoSmithKline R&D, Stevenage, Hertfordshire, SG1 2NY (UK)
E-mail: philip.g.humphreys@gsk.com
[b] M.A. Clegg, Prof. N. C. O. Tomkinson
WestCHEM, Department of Pure and Applied Chemistry
Thomas Graham Building, University of Strathclyde
295 Cathedral Street, Glasgow, G1 1XL (UK)

Mike Clegg studied for his Masters in Chemistry at the University of Bristol where he graduated with first class honours and a School of Chemistry Commendation in 2016. He is currently studying for his PhD as part of the GSK/University of Strathclyde collaborative PhD scheme where his research focuses on the design and synthesis of novel non-BET bromodomain chemical probes for target validation.

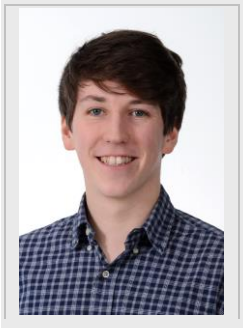

Nick Tomkinson was born in St Andrews, Scotland in 1969. He studied Chemistry at The University of Sheffield and received his BSc in 1992 and PhD in 1996 under the supervision of Dr D. Neville Jones and Professor Jim Anderson. After postdoctoral studies with Professor Tim Willson at GlaxoSmithKline, Research Triangle Park, North Carolina (1996–1998), he was appointed to the staff at Cardiff University in 1999. In June 2011 he took up a position in the Department of Pure and Applied Chemistry at the University of Strathclyde. His research is split into two distinct areas: The development of practical synthetic methodology and the preparation of tool compounds of biological relevance. The approach to discovery in each of these areas is driven by mechanistic knowledge and understanding.

Rab Prinjha currently leads the merged Epigenetics DPU supporting both the ImmunoInflammation and Oncology Therapy Area Unit portfolios. Prior to leading the Epinova DPU he led the Target Progression department with responsibilities for target selection, validation and epigenetic compound characterisation along with coordinating academic collaborations. He joined Epigenetics from the II-virtual group which was responsible for implementing the externalisation and portfolio diversification strategy of the TA. Previously he led a Target Validation group in the Neurology CEDD focussed on neurodegeneration. In addition to advancing many programs while in Neurology he cloned a novel inhibitor of CNS regeneration called Nogo-A and led this program from gene cloning to Candidate Selection and into clinical trials. Rab cofounded the GSK Biology Council and is a member of the OpenTargets and Milner Therapeutics Consortium Governance Boards and sits on the MRC PSMB Board. He was a member of the Padlock Board until their acquisition by BMS. He is a Fellow of the Royal Society of Biology and was elected to the Academy of Medical Sciences in 2017. Rab joined GSK from academia including a post-doc in developmental neuroscience at Guy's Hospital and PhD in molecular biology of the cell cytoskeleton at UCL.

Phil Humphreys studied Biochemistry and Biological Chemistry at the University of Nottingham and received his D.Phil. from the University of Oxford under the supervision of Prof. David Hodgson in 2007. Following postdoctoral research with Prof. Larry Overman at the University of California, Irvine he joined GlaxoSmithKline, Stevenage in 2009 as a medicinal chemist in the Immune Memory DPU. He transitioned into the Epigenetics DPU in 2010 where he led chemistry teams and programmes on a variety of epigenetic targets, particularly in the bromodomain space. In 2017 he was elected as a GSK Fellow and was also the recipient of the 2017 European Federation for Medicinal Chemistry Prize for a Young Medicinal Chemist in Industry. In 2018 he joined the Pulmonary Vascular Injury DPU as the Head of Medicinal Chemistry where he has worked since.

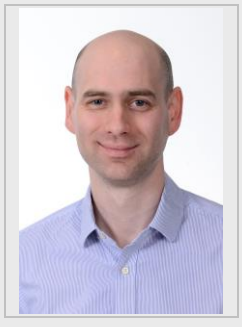

and selectivity; 3) provide sufficient data to assign phenotypic results to an original structure or a well characterized derivative; and 4) provide cellular activity data to answer a hypothesis on the role of the target. Consequently, the following criteria are used within GSK as guidelines when designing bromodomain chemical probes to ensure all 4 of these objectives can be fulfilled.

1. pIC_{50} ≥7 (IC_{50} <100 nM) against target in a biochemical assay.
2. > ×100 selective against BET bromodomains (for which a strong biological phenotype is known).
3. > ×30 selective against other non-BET bromodomains.
4. Understanding of broader off-target activity.
5. Suitable solubility and permeability to ensure exposure at target site.
6. Cellular activity at <1 μM concentrations (pIC_{50} > 6).
7. Be accompanied by a structurally related negative control.
8. Expand the structural diversity of bromodomain chemical probes.

Pivotal to the applicability of a chemical probe is the allocation of an observed phenotype to target inhibition. Therefore, when developing small molecule bromodomain inhibitors, selectivity is heavily scrutinized, in particular against the BET bromodomain family for which a strong biological phenotype is known. From GSK's own experience, a 100-fold selectivity window is required for adequate biological interpretation. Additionally, small molecule inhibitors will inherently hit a multitude of biological targets. Moving forward, the advent of chemoproteomic profiling allows for more holistic compound profiling,[12] however until then, any additional information regarding off-target affinity that can be obtained, typically via screening against internal panels available to the institute or via a CEREP panel, is desired.

In the absence of infinite off-target screening, the presence of equally well characterized structurally related negative control compounds, and additional inhibitors of different chemotypes help

mitigate this issue, providing further bias to suggest an observed phenotype is due to target inhibition.

The advanced understanding of BET bromodomain pharmacology and the small molecules progressing through clinical trials, is in part due to the ready availability of high quality chemical probes for these targets. With BCP dysregulation implicated in a number of disease states, there has been a surge of interest in non-BET bromodomain chemical probes to aid target validation of these epigenetic reader modules. This area was reviewed previously in 2015 by 3 of the corresponding authors.[13] Since this review, however, the field has progressed rapidly with a number of new chemical probes being developed and disclosed (**Figure 2**). The quality of non-BET bromodomain chemical probes, and the variety of chemotypes included, has also advanced dramatically, reflecting the awareness and uptake of the guidelines mentioned previously. The generation of high quality chemical probes, and the structural information typically obtained during their development, has also facilitated the development of more sophisticated bifunctional chemical biology tools. These include bivalent inhibitors, proteolysis targeting chimeras (PROTACs) and photoaffinity probes which can provide additional information into the validation of biological targets.[14]

All non-BET bromodomain tool molecules disclosed between December 2015 and October 2018 shall be reviewed here with close attention to the aforementioned criteria, noting any opportunities for future probe development and their applicability as chemical probes for target validation. For reader clarity, all bromodomain inhibitors have been drawn (where possible) with the acetylated lysine mimetic in the top-left/bottom-left corner and, when available, a crystal structure of the inhibitor bound to the target protein has been included.

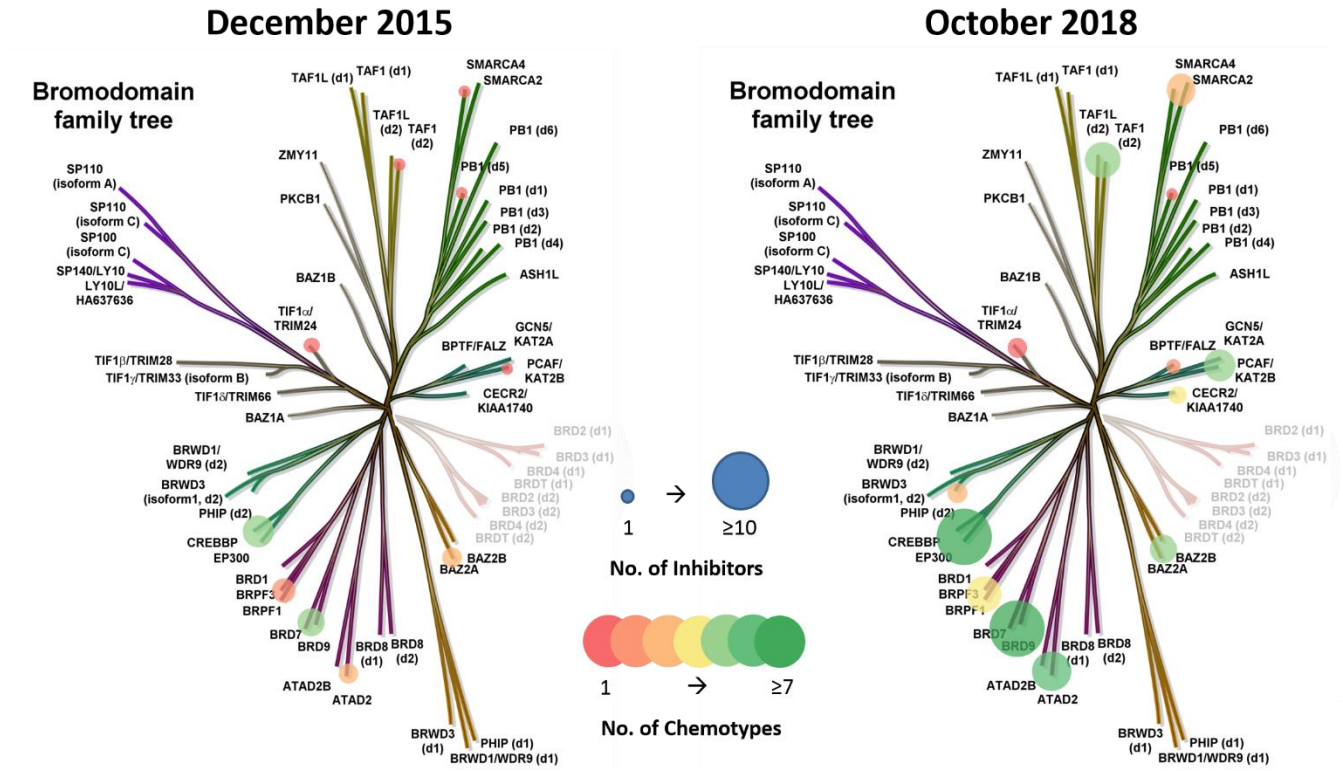

Figure 2. Bromodomain phylogenetic tree highlighting the number of different inhibitors (size of spot) for a given bromodomain and the number of unique chemotypes (colour of spot) presented by these inhibitors. BET subfamily has been greyed out for clarity.

2. Typical Non-BET Bromodomain Inhibitors

CECR2

As the name suggests, cat eye syndrome chromosome region candidate 2 (CECR2) has an active role in human disorder cat eye syndrome, which in turn is attributable to eye, heart, kidney, face and skeletal malformations. CECR2 is predominantly expressed in the nervous system, with CECR2 deletion being associated with neural tube defects. CECR2 has also been shown to inhibit γ-H2AX following DNA double strand breaks, and consequently is thought to play a role in DNA damage response.[15]

At the end of our previous review, CECR2 had no reported chemical probes, with only mildly potent (pIC_{50} = 5.8-6.6) pan inhibitors available at that time. Since then, the first CECR2 chemical probes have been developed and disclosed.

Collaborative work between Novartis and the SGC has led to the development of NVS-CECR2-1 (**1**), a potent and selective CECR2 bromodomain inhibitor. **1**'s potency for CECR2 was demonstrated using an Alpha screen assay (pIC_{50} = 7.3), and was reported to be inactive against a bromodomain panel of 48 targets, highlighting its desired selectivity, although no data is provided.[16] Furthermore, **1** reports good selectivity against pharmacologically relevant off targets where tested, showing no activity in kinase, protease and receptor panels, although again no data is provided. Additionally, **1** is accompanied by a structurally similar negative control in the form of NVS-CECR2-C which is inactive against CECR2, although no structure is reported. The permeability of **1** is not provided, but fluorescence recovery after photobleaching (FRAP) data indicates cell penetration and cellular activity at 0.1 µM. Finally, poor solubility is mentioned but no data provided. Bromodomain selectivity, in particular over the BET subfamily. Is not specified, potentially limiting the application of **1** as a chemical probe for CECR2, however this likely will be addressed when the work is published.

Crawford and co-workers. have also disclosed a potent and selective inhibitor of CECR2, known as GNE-886 (**3**). An initial screen of 600 compounds led to the N-methyl pyrrolopyridinone hit compound **2** which was prioritised due to its selectivity over the BET bromodomains (BRD4 pIC_{50} <4.7), and minor selectivity over BRD9 (×2), despite showing a greater potency towards TAF1 than CECR2. Structure based lead optimization was used to improve the selectivity over BRD9 and TAF1, resulting in **3**, which displayed potency for CECR2 (pIC_{50} = 7.8). **3** also demonstrated >1000-fold selectivity over BET bromodomains (pIC_{50} <4.7), 100-fold selectivity over BRD9 (pIC_{50} = 5.8), and 80-fold selectivity over TAF1 (pIC_{50} = 5.9) which were all measured within a TR-FRET assay. Similarly, **3** appeared selective against a panel of 35 diverse kinases, with no kinase inhibited >20% at 1 µM. Moreover, **3** is soluble (609 µg/mL) and the displacement of CECR2-Zs Green fusion protein from chromatin was measured (pEC_{50} = 6.4), demonstrating permeability and cellular activity. Unfortunately, **3** does not have a known structurally related negative control.[17]

Finally, collaborative work between Takeda and the SGC has led to the discovery of TP-238 (**4**), a reported dual chemical probe for CECR2 and BPTF.[18] **4** displayed potency for both CECR2 (pIC_{50} = 7.5) and BPTF (pIC_{50} = 6.5) in an Alpha screen

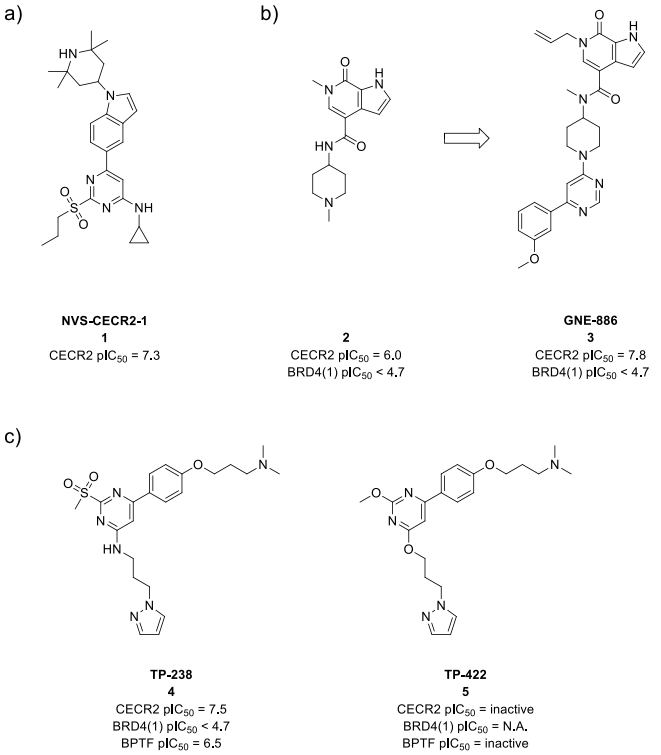

Figure 3. a) Structure of CECR2 chemical probe **1**; b) Structure of CECR2 chemical probe **3** and initial hit compound **2**; c) Structure of CECR2/BPTF inhibitor **4** and accompanying negative control **5**.

assay and, whilst no solubility or permeability data is provided, cellular activity was demonstrated at submicromolar concentrations in a NanoBRET assay for both CECR2 and BPTF. Micromolar potency against BRD9 (pIC_{50} = 5.9) is reported as the closest off-target bromodomain inhibition although no further data is provided. Additionally, no activity at 1 µM was observed against a panel of 338 kinases, providing insight into **4**'s potential off-target activity. TP-422 (**5**), an accompanying negative control was also disclosed and is reported to be completely inactive against CECR2 and BPTF, although no mention of concentration is provided. Hopefully further data and information surrounding the discovery of **4** will be disclosed when the work is published. In particular, data regarding BET potency and the corresponding selectivity would help in the application of **4** as a dual CECR2/BPTF probe.

1, **3** and **5** offer three much needed inhibitors for the CECR2 bromodomain. Their structurally differentiated chemotypes, and an accompanying negative control, provides promise for the target validation of CECR2's bromodomain and the assignment of any observed phenotype, although thorough target validation would benefit from further equally characterized inhibitors.

PCAF/GCN5

P300/CBP-associated factor (PCAF) and general control non-depressible 5 (GCN5) are two HAT proteins that have been linked with diseases spanning across a diverse range of therapeutic areas, including oncology,[18–20] neuro-degeneration,[21,22] HIV infection,[23–25] and inflammation pathways.[26] Despite being mutually exclusive proteins, the highly homologous amino acid sequence shared between them (~73%) and their bromodomains

in particular, suggests targeting one selectively over the other is unlikely.

By the end of 2015, the PCAF/GCN5 chemical tool landscape was limited, with only one PCAF/GCN5 inhibitor having been disclosed. Moreover, the reported inhibitor possessed µM potency (pIC_{50} = 5.8), thus requiring further optimization. During the past 3 years, multiple PCAF/GCN5 inhibitors and chemical probes have been disclosed.

In 2016, three patent applications from Genentech and Constellation Pharmaceuticals were released disclosing a number of highly potent PCAF/GCN5 dual inhibitors spanning three different chemotypes. Exemplified by compounds **6**, **7** and single unknown diastereomer **8** (**Figure 4a**), [27–29] (the most active analogues from each series) each chemotype demonstrated significant improvements in PCAF/GCN5 potency compared to the previously reported PCAF inhibitors.[13] Due to the nature of patent applications, little is known about the selectivity, permeability, solubility and cellular activity of any of the disclosed compounds, thus, it is impossible to comment on their ability to function as PCAF/GCN5 chemical probes.

Developed independently, yet bearing a striking similarity to compounds disclosed by Genentech and Constellation Pharmaceuticals (e.g. **6**)[27], researches at GSK published GSK4027 (**10**) as a selective and potent PCAF/GCN5 chemical probe (**Figure 4b**). Starting from a screening of ~30000 known and potential acetyl lysine mimetic containing compounds, an initial pyridazinone scaffold, demonstrating moderate potency (pIC_{50} = 4.8) and good ligand efficiency (0.37), was optimized by iterative SAR to develop **10**. X-ray crystallography was used to drive the optimization of hit compound **9** and to identify a number of hydrogen bond interactions between **9** and the bromodomain of PCAF (**Figure 4d**). These include the expected hydrogen bond between the carbonyl group and the side chain NH_2 group of Asn803, and a shorter water mediated hydrogen bond to Tyr760. More interestingly was the observation that the halogen group was acting as the methyl mimetic, and not the expected methyl group, and the identification of Glu756 as a key acidic residue found in the ZA channel, absent in BET bromodomains, from which **last time I'll highlight this. Could say..... from which high selectivity of 10....** over the BET subfamily was achieved. Utilizing a TR-FRET assay, **10** demonstrated good potency against PCAF (pIC_{50} = 7.4) and >1000-fold selectivity over the BET subfamily (BRD4(1) pIC_{50} <4.3). The selectivity of **10** was further investigated *via* a BROMOscan panel ultimately confirming **10**'s high selectivity, demonstrating ≥18000-fold selectivity over the BET family of bromodomains and ≥70-fold selectivity over the other remaining bromodomains, with an exception of the highly homologous GCN5 where equipotency was displayed. Additionally, **10**'s selectivity over a collection of pharmacologically relevant off-targets was also investigated with cross screening against a panel of 53 biochemical and phenotypic assays showing no activity <3 µM. **10** possesses good permeability (500 nm/s) and solubility (149 µg/mL) and demonstrated cellular target engagement of PCAF (pIC_{50} = 7.2) through the use of a NanoBRET assay, providing convincing

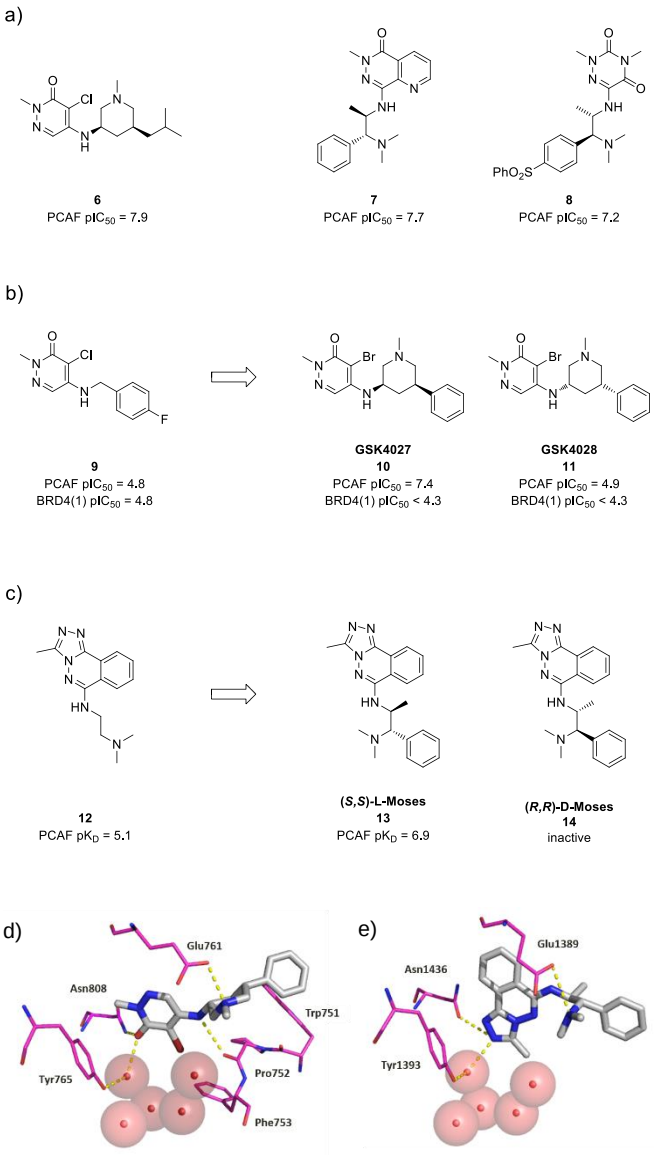

Figure 4. a) Structures of PCAF/GCN5 inhibitors **6**-**8**; b) Structures of PCAF/GCN5 chemical probe **10**, accompanying negative control **11** and initial hit compound **9**; c) Structures of PCAF/GCN5 chemical probe **13**, accompanying negative control **14** and initial hit compound **12**; d) Crystal structure (PDB: 5MLJ) of **10** (grey) bound to human bromodomain GCN5 (purple); e) Crystal structure (PDB: 5TPX) of **13** (grey) bound to plasmodium falciparum bromodomain GCN5 (purple).

evidence to support its ability to reach the target site. **8** was also accompanied by GSK4028 (**11**) an enantiomeric negative control (PCAF pIC_{50} = 4.9).[30]

Similarly, L-Moses (**13**), another selective and potent PCAF/GCN5 inhibitor, has recently been reported as a chemical probe for PCAF/GCN5 (**Figure 4c**).[31] The triazolopyridazine scaffold, found in promiscuous bromodomain inhibitor bromosporine[32], was used as a starting point. Introduction of small amine groups were used to exploit the characteristically narrow PCAF ZA channel and to establish the acid/base interaction with Glu756 discussed previously (**Figure 4e**), from which selectivity over the BET subfamily can be attributed. Differential scanning fluorimetry (DSF) identified hit compound **12** from which further

iterative SAR was conducted, ultimately resulting in **13**. **13** displayed good potency against PCAF (pK_d = 6.9) and GCN5 (pK_d = 6.2) as demonstrated by isothermal titration calorimetry (ITC). Additionally, **13** also displayed good selectivity against BET bromodomains (>×4500 over BRD4) and the remaining non-BET bromodomains, measured using DSF. **13** is soluble (>72 µg/mL), permeable in MDCK-MDR1 cells (100 nm/s), and was shown to displace NanoLuc-tagged full-length PCAF from Halo-tagged histone H3.3 within cells at 5 µM. A structurally related negative control for **13** is reported in the form of its inactive enantiomer D-Moses (**14**).

The pharmacophore similarity between the molecules disclosed by Genentech/Constellation Pharmaceuticals, GSK and the SGC is striking. In particular, the HBD separated by two atoms from a basic amine and the pendant lipophilic group are seen in all the highlighted PCAF/GCN5 inhibitors. This raises concern for potential common off-targets and is an issue that will hopefully be addressed with new chemotype PCAF/GCN5 chemical probes in the future. Additionally, a lack of selectivity between PCAF and GCN5 prevents the assignment of any phenotype to a single bromodomain, and dissection of their individual roles in healthy/disease state modulation.

BPTF

BPTF (bromodomain and PHD finger transcription factor), aka FALZ, has been identified as an oncology target, being associated predominantly with a wealth of cancers such as colorectal,[33] bladder,[34] melanoma[35] and leukemia.[36] A lack of any reported BPTF bromodomain inhibitors has resorted in a poor understanding of BPTFs role in these diseases. Recently however, Urick and co-workers have reported the first BPTF bromodomain inhibitor, arylurea AU1 (**15**) (**Figure 5a**). A library of 229 small molecules was screened simultaneously against BRD4(1) and the bromodomain of BPTF using protein-observed ^{19}F-NMR (PrOF NMR), ultimately leading to **15** and two other selective hits, with follow up ITC experiments confirming **15**'s potency (BPTF pK_D = 5.6) and selectivity for BPTF over BRD4(1) (negligible chemical shift changes at up to 160 µM). Kinase inactivity, and activity in 'cell culture' is reported, although, along with solubility and permeability, no data is provided. Binding of arylurea inhibitors to BPTF has been correlated to a benzene ring with a meta-substituted carbonyl. Docking of **15** into the bromodomain of BPTF supports this hypothesis, with π-π interactions to Phe2887 and hydrogen bonds to Asn2881 observed, although crystallography is required to confirm this.[37,38] Although substantial further development into BPTF inhibitors is required to enable the target validation of BPTF's bromodomain, **15** demonstrates the BPTF bromodomain is ligandable with small molecules, and acts as a lead molecule for further optimization.

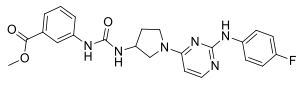

AU1
15
BPTF pK_D = 5.6

Figure 5. Structure of BPTF inhibitor **15**.

CREBBP/EP300

CREBBP (CREB binding protein) and EP300 (E1A-associated protein p300) are adenoviral E1A-binding proteins involved in multiple cellular processes, functioning as HATs and transcription co-factors. Since their discovery, both have been implicated in a variety of cancers such as prostate cancer,[39] acute myeloid leukemia,[40] and Rubinstein-Taybi syndrome.[41] The highly homologous bromodomains of these closely related proteins suggests individual inhibition of each is difficult.

The CREBBP/EP300 chemical tool repertoire is one of the most extensive of the non-BET bromodomains. This was the case 3 years ago during our previous review where two submicromolar potency compounds were discussed (pK_D = 6.8 & 7.7). Since that review, a number of other CREBBP/EP300 inhibitors have been developed, including multiple with nM potencies (pIC_{50} = 8.0-9.2), exemplifying the dramatic advancements in the field.

Crawford and co-workers have reported GNE-272 (**17**), as a potent CREBBP/EP300 inhibitor (**Figure 6a**). A thermal shift assay was used to screen CREBBP against a diverse set of compounds with assigned "lead-like" properties.[42] Subsequent dose response characterization of the most potent hits (ΔT_m >1 ºC) followed, ultimately leading to initial hit compound **16** being selected for further optimization, due to possessing good LE (0.47) and ~100-fold selectivity over BET bromodomains (BRD4(1)). X-ray crystallography identified the N-acetyl group as the acetylated lysine mimetic with the amide carbonyl forming a hydrogen bond interaction with Asn1168 and water-mediated hydrogen bond interactions with Pro1110 and Tyr1125. Additionally, van der Waals interactions between the phenyl ring and the LPF shelf (Leu 1109, Pro110 and Phe1111) were observed, whilst the pyrazolopiperidine core was shown to occupy the space between the gatekeeper residue (Val1174) and Leu1120. Guided SAR and optimization of permeability and mouse liver microsomal stability ultimately delivered compound **17**. **17** demonstrated good potency for CREBBP (CREBBP pIC_{50} = 7.7), and 630-fold selectivity over BET bromodomains (BRD4(1) pIC_{50} = 4.9) in a TR-FRET assay. **17**'s selectivity against other non-BET bromodomains was partially investigated, displaying >600-fold selectivity against 10 BCPs. **17** displayed good permeability (P_{appA-B} = 150 nm/s) and demonstrated cellular activity at submicromolar concentrations (CREBBP pIC_{50} = 6.4) in a NanoBRET assay.

Since the disclosure of **17**, Genentech have optimized the scaffold further to produce chemical probe GNE-781 (**18**) (**Figure 6a**). Seeking to further improve potency for CREBBP and selectivity over the BET sub-family, the aniline nitrogen of **17** was constrained into a bicyclic tetrahydroquinoline (THQ) to further disfavour the planar binding conformation adopted by **17** in BRD4(1). Additionally, structure-based optimization was utilized to target the LPF shelf and BC loop (**Figure 6c**). Finally, switching to a methyl urea acetylated lysine mimetic to introduce an additional H-bond donor, and thus reduce CNS penetration, resulted in **18**.[43] As discussed, **18** displayed excellent potency for CREBBP (pIC_{50} = 9.0) and an improved selectivity over the BET family (pIC_{50} = 5.3). Additionally, **18** showed selectivity over the non-BET bromodomains (>×5000), as demonstrated by a DiscoverX BROMOscan (40 bromodomains) panel, as well as against kinase (no inhibition >10% at 1 µM), CEREP off-target (no inhibition >39% at 10 µM), and cytochrome p450 (no inhibition at 1 µM) panels. Target engagement was also demonstrated using a NanoBRET assay with **18** displaying excellent potency (CREBBP pIC_{50} = 8.2) and demonstrating cellular permeability.

Additionally, **18** was also shown to possess acceptable PK parameters in mouse, rat, dog and monkey, offering promise for its use within an *in vivo* setting also. The quality of **18** as a chemical probe for CREBBP/EP300 was reflected in the target validation accomplished utilizing **18**. Inhibition of the CREBBP bromodomain was shown to modulate CREBBP-dependent MYC expression and supress MOLM-16 tumour growth. Additionally, **18** was used to confirm the interaction of CREBBP with FOXP3, a transcription factor essential for immune homeostasis,[44] providing invaluable target validation of the CREBBP bromodomain, and proposing CREBBP bromodomain inhibition as a novel avenue for cancer immunotherapy.

Genentech subsequently demonstrated the transferability of the THQ-CF_2H pyrazole shelf group, responsible for **18**'s excellent CREBBP/EP300 potency and selectivity, by designing and optimizing two additional CREBBP/EP300 inhibitors, **19** and **20**, with benzimidazolone and azaindole cores respectively. As predicted, the CREBBP potency was maintained for both **19** and **20**, along with 300-fold and 1000-fold selectivity over the BET bromodomains respectively. Additionally, both compounds demonstrated >1000-fold selectivity over other non-BET bromodomains and cellular activity within a MYC expression assay, with **21** also exhibiting low clearance (18.2 mL min^{-1} kg^{-1}) and moderate bioavailability (52%) in mice.[45]

Using SGC-CBP30 (**21**) as a start point, Pfizer have developed PF-CBP1 (**22**) (Figure b) through the use of structural based design with existing CREBBP and BRD4 crystal structures (**Figure 6d**).[46] **22** showed good potency for CREBBP (pIC_{50} = 6.9) and weak BRD4(1) potency (pIC_{50} = 4.7), revealing a >100-fold selectivity. The benzoimide N-3 nitrogen was shown to form a water mediated hydrogen bond interaction with Pro82 in BRD4. Therefore, to further improve CREBBP/EP300 selectivity, the benzimidazole core of **22** was converted to an azoindole group in an attempt to remove this interaction and point the nitrogen towards solvent, ultimately leading to PF-CBP2 (**23**). **23** also showed good potency for CREBBP (pIC_{50} = 6.9) and weak BRD4(1) potency (pIC_{50} = 4.7). Additionally, **23** was also screened against a further 30 bromodomains using the DiscoverX BROMOscan panel with good selectivity being observed throughout, excluding BAZ2A (>80% inhibition at 10 µM), although no K_D values have been determined. Additionally, a clean polypharmacology profile (pIC_{50} <5.0) was also observed across a 19 component CEREP panel. Although **23** appears

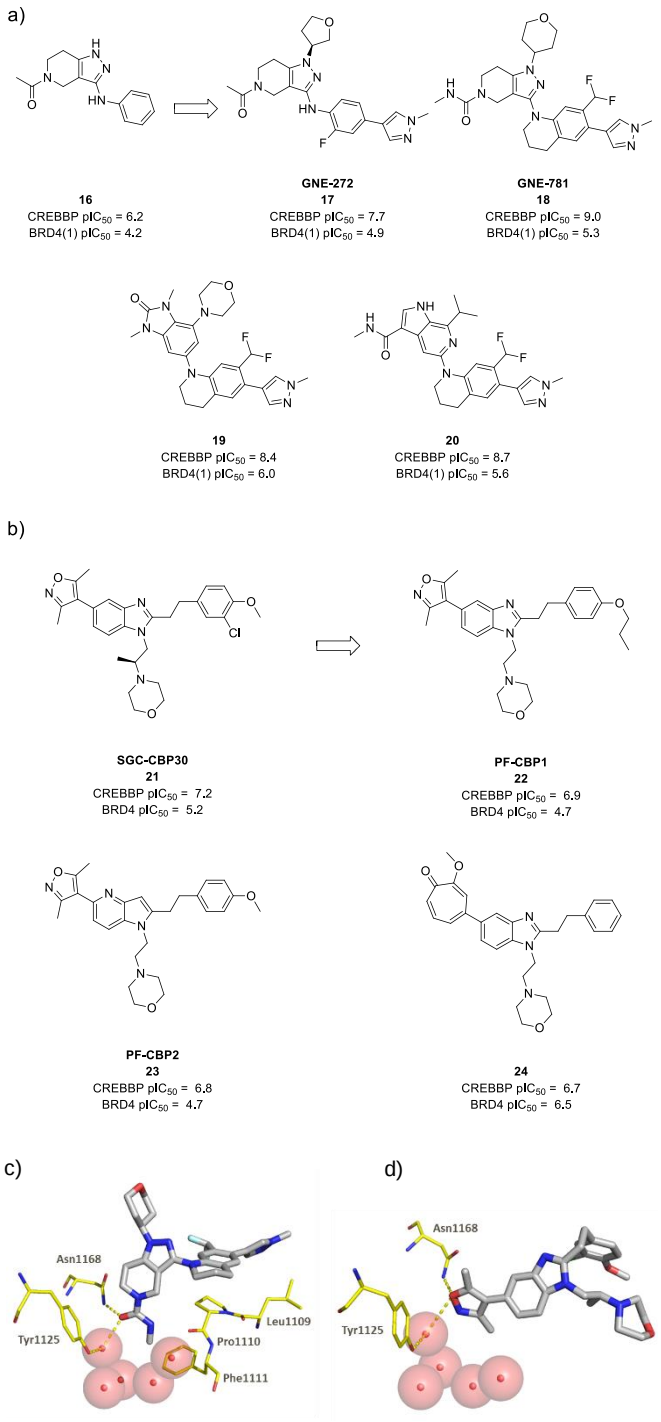

Figure 6. a) Structure of CREBBP chemical probes **17** and **18**, initial hit compound **16** and additional CREBBP inhibitors **19** and **20**; b) Structures of CREBBP inhibitors **21**-**24**; c) Crystal structure (PDB: 5W0E) of **18** (grey) bound to human bromodomain CREBBP (yellow); d) Crystal structure (PDB: 4NR7) of **21** (grey) bound to human bromodomain CREBBP (yellow).

permeable (68 nm/s) no cellular activity data is reported. Furthermore, measured K_Ds for the most active bromodomains at 10 µM, in particular BAZ2A, would help confirm **23**'s selectivity and thus any phenotypic assignment from the probe. Pfizer also demonstrated the potential for N-ethyl pyridinone warheads, and from their photoaffinity probe work,[47] tropolone mimetics such as

24, helping to expand the SAR further and offering new avenues for CREBBP/EP300 chemical probe development.

Two CREBBP/EP300 inhibitors have been discovered by Xiang and co-workers, based around a 1-(1*H*-indol-1-yl)ethanone chemotype (**Figure 7a**).[48] Commencing with a fragment based virtual screen, fragment **25** was subsequently optimized to deliver inhibitor **26** utilizing X-ray crystallography driven SAR. The carbonyl of the carboxyl group was shown to form a water mediated hydrogen bond to Arg1173 and vital to CREBB potency. Thus, an amide linker and an aromatic ring were introduced to increase the rigidity of the chain and optimize this interaction. Utilizing an Alpha screen assay, **26** was shown to demonstrate good potency for CREBBP (pIC_{50} = 7.4) and to be highly selective over the BET subfamily (pIC_{50} < 4.7) and a selection of five other non-BET bromodomains (all pIC_{50} < 4.7). Although no permeability or solubility data is reported, a lack of inhibition effect against LNCaP and 22Rv1 cells is attributed to poor cellular permeability, due to the highly polar carboxyl group. Consequently, ester derivative **27** was synthesized and demonstrated reasonable potency for CREBBP in biochemical (pIC_{50} = 6.4) and cellular (pIC_{50} = 5.7) assays. Compound **26** poses itself as a new chemotype for CREBBP/EP300 inhibitor development but would benefit from further selectivity characterization, in particular against other non-BET bromodomains and pharmacological off-targets. Additionally, it is unclear whether **27** itself is the active species responsible for inhibition of CREBBP within the cellular assay, or if the ester is hydrolyzed within the cells to generate **26** in a prodrug fashion.

XDM-CBP (**29**) has also been published as an inhibitor of CREBBP/EP300, optimised from the core fragment structure (**28**) of recently published BET inhibitor XD14 (**Figure 7b**).[49] Utilizing a combination of computational methods, along with X-ray crystallography and ITC, **29** was developed with micromolar potency for CREBBP (pK_D = 6.6) and good selectivity (×150) over BET bromodomains (BRD4(1) pK_D < 4.4). Key to this drop in BET potency was the introduction of hydroxy groups to the naphthalenyl ring which provided additional intramolecular hydrogen bonds (**Figure 7d**), and consequently an increased rigidity, making the conformational change to adapt to the acetylated lysine binding site of BRD4(1) energetically disfavoured. **29** appeared selective (>×40) against a 40 bromodomain DiscoverX bromoKdELECT assay, with the exception of BRD7 (BRD7 pK_D = 5.3) and BRD9 (BRD9 pK_D = 5.5) where 10-fold selectivity was observed. Selectivity against pharmacologically relevant off-targets is currently unknown for **30**, as is the potential for cellular activity at submicromolar concentrations. Nevertheless, **29** provides a promising ligand efficient (LE = 0.33) fragment for future optimization.

Further optimization around a previously reported CREBBP inhibitor, I-CBP112 (**30**),[50] has led to the discovery of TPOP146 (**31**) (**Figure 7c & e**).[51] Starting from an initial library of 48 2,3,4,5-tetrahydro-1,4-benzoxazepine scaffold containing compounds, DSF was utilized to identify the racemate of previously discussed inhibitor **30** as an initial hit compound. Comprehensive SAR investigation around the 2,3,4,5-tetrahydro-1,4-benzoxazepine

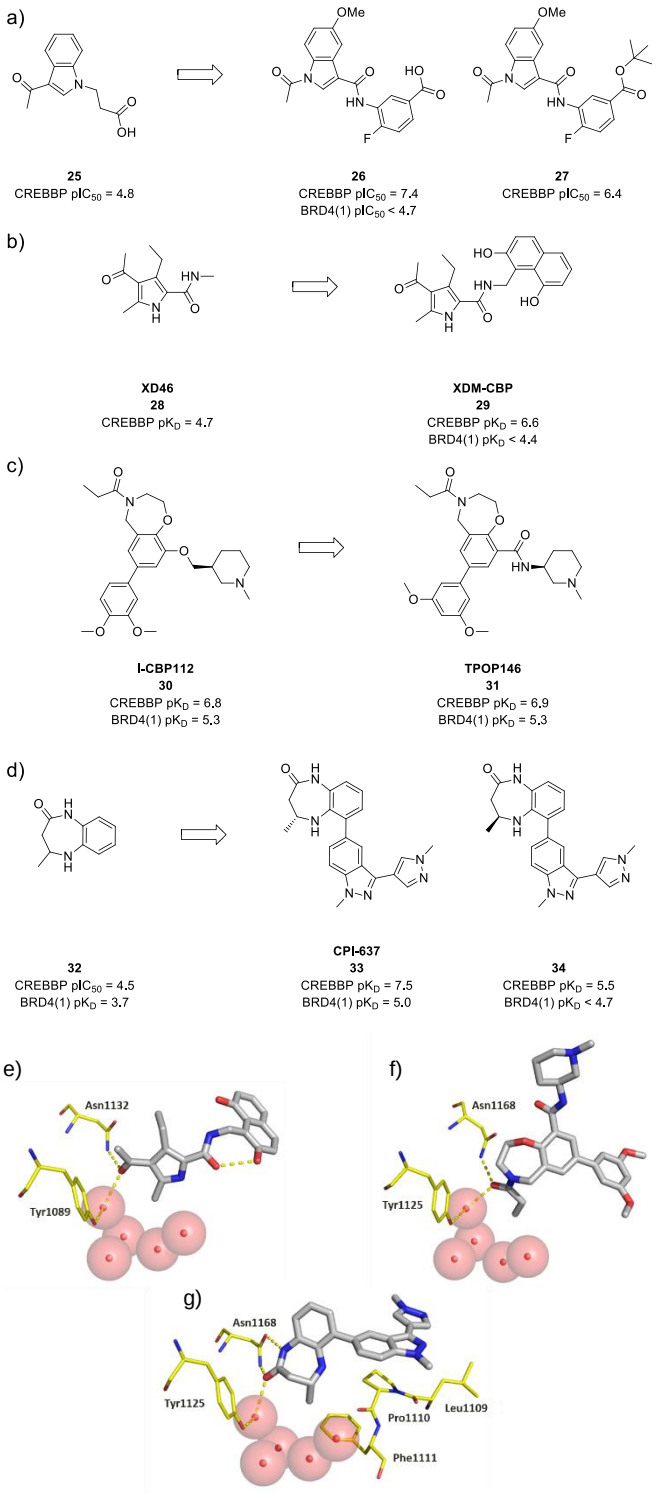

Figure 7. a) Structure of CREBBP inhibitors **26** and **27**, and initial hit compound **25**; b) Structure of CREBBP inhibitor **27** and initial hit compound **28**; c) Structure of CREBBP inhibitor **31** and starting point **30**; d) Structure of CREBBP inhibitor **33**, accompanying negative control **34** and initial hit compound **32**; **e**) Crystal structure (PDB: 5NU5) of **29** (grey) bound to human bromodomain EP300 (yellow); f) Crystal structure (PDB: 5J0D) of **31** (grey) bound to human bromodomain CREBBP (yellow); g) crystal structure (5I8G) of **33** (grey) bound to human bromodomain CREBBP (yellow).

scaffold ultimately led to **31**. Using ITC, **31** demonstrated potency for CREBBP (pK_D = 6.9) and 30-fold selectivity over BRD4(1) (pK_D

= 5.3). Furthermore, **31** appeared selective against a further 44 bromodomains when investigated via DSF, although it should be noted, DSF varies from protein to protein and as such should be treated with caution. Cellular activity was demonstrated using a modified FRAP assay, in which 1 µM concentrations produced a reduced recovery half-life. Despite improved non-BET bromodomain selectivity compared to **30**, again, only moderate selectivity over the BET subfamily limits the applicability of benzoxazepine CREBBP/EP300 inhibitors.

CPI-637 (**33**), a CREBBP/EP300 inhibitor based around a benzo[1,4]-diazepin-2-one scaffold, has been reported by Genentech and Constellation Pharmaceuticals (**Figure 7d**).[52] A fragment screening of ~2000 compounds in a thermal shift assay was utilized to identify hit compound **32**, chosen for displaying potency at CREBBP (pIC_{50} = 4.5) and 7-fold selectivity over the BET subfamily. X-ray crystallography identified the lactam portion of the benzo[1,4]-diazepin-2-one to be functioning as the KAc mimetic, with the expected hydrogen and water mediated hydrogen bond interactions to the conserved Asn and Tyr respectively observed. An additional hydrogen bond interaction was also observed between the lactam NH and the carbonyl of the conserved Asn (**Figure 7g**), whilst the 4-methyl group was shown to occupy the hydrophobic binding pocket. Substitution at the 6 position with indazoles was shown to fill space above Pro1110 and the Pro/Arg cleft to provide additional hydrophobic interactions and an accompanying boost in CREBBP potency, eventually leading to **33**. **33** showed potency at CREBBP (pIC_{50} = 7.5) and >200-fold selectivity over the BET subfamily and 6 other non-BET bromodomains. Activity was however observed against BRD9 (pIC_{50} = 6.1). Moreover, **33** demonstrated potency for CREBBP within a cellular assay ($pIEC_{50}$ = 6.5) and was accompanied by a structurally related negative control (CREBBP pIC_{50} = 5.5) in the form of its opposite enantiomer. No data on other pharmacological off-targets is provided, and further non-BET selectivity characterization would be beneficial.

The discussed compounds add extra value and increased diversity to the already extensive CREBBP/EP300 chemical probe tool box. In particular, **18** offers a step change in potency and BET selectivity from previously disclosed CREBBP/EP300 probes. The advanced CREBBP/EP300 tool box for target validation is also reflected in the number of recently disclosed CREBBP therapeutic patents (**Figure 8**). Genentech and Constellation Pharmaceuticals have released three patents disclosing a range of CREBBP/EP300 inhibitors based around the tetrahydro-pyrazolopyridine scaffold seen previously, and a dihydro-benzodiazepinone group. The most potent compound of each chemotype, **35** and **36**, are shown as representative examples.[53–55] **35** displays excellent potency for CREBBP (pIC_{50} = 9.1) and is reported to be active within a cellular MYC assay (pIC_{50} = 8.1). Similarly, **36** shows excellent potency for CREBBP (pIC_{50} = 9.2) and is active within a cellular MYC assay (pIC_{50} = 8.0). Additionally, BET potency data is reported for **36**, highlighting its high selectivity (×1000). Similar data is reported for **37** which is also potent at CREBBP in biochemical (pIC_{50} = 8.5) and cellular MYC assays (pIC_{50} = 8.0) and is selective (×1000) over the BET subfamily. Due to the nature of patents, however,

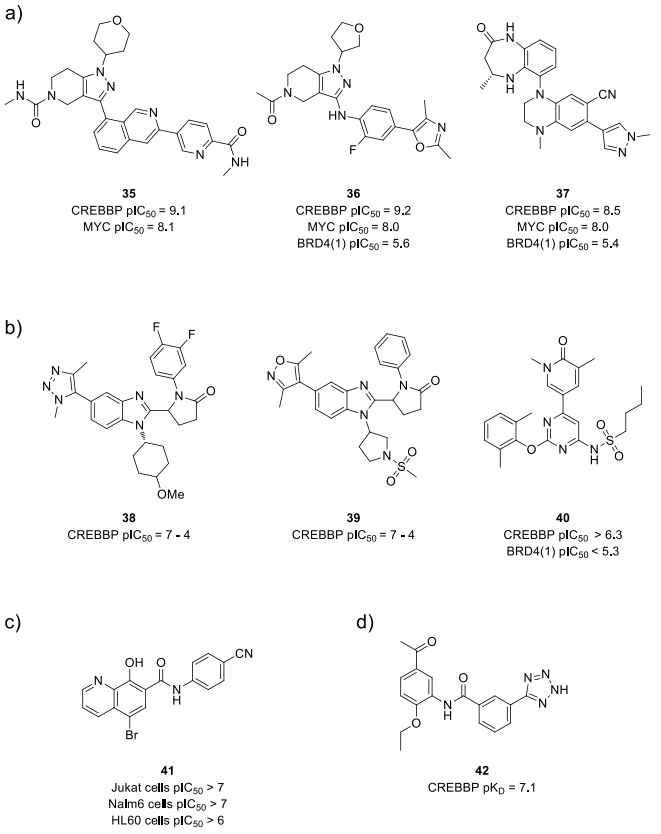

Figure 8. a) Structure of reference patented CREBBP inhibitors **35**-**37**; b) Structure of reference patented CREBBP inhibitors **38**-**40**; c) Structure of reference patent CREBBP inhibitor **41**; d) Structure of reference patent CREBBP inhibitor **42**.

no further information is provided for either compound. Likewise, Cellcentric have released two patents on CREBBP/EP300 inhibitors based around triazole and isoxazole KAc mimetics.[56,57] A representative example of each chemotype, **38** and **39**, are shown. Although no data was provided, both are reported to have potencies between 100 nM-100 µM. A patent on CREBBP/BRD4 dual inhibitors was also released by Celgene disclosing a range of CREBBP inhibitors.[58] Although no specific potency data was disclosed, ranges of potency were provided and a selective CREBBP example **40** is shown. Stanford Junior University have also disclosed a number of CREBBP/EP300 inhibitors via patent application, in which ranges of cell viability data were disclosed against three cell lines (HL60, Jukat and Nalm6).[59] **41** was chosen as a representative example, displaying pIC_{50} >7 in Jukat and Nalm6 cell assays and a pIC_{50} >6 in HL60 cell assay. Finally, a patent disclosing a wealth of CREBBP/EP300 inhibitors was released by the University of Zurich.[60] The most potent CREBBP inhibitor (CREBBP pK_D = 7.1) **42** is shown as a representative example.

BRPF1/2/3

Some of the more well understood non-BET BCPs are the bromodomain and PHD finger-containing protein family

(BRPF1/2/3). BRPF1/3 & BRPF2 (aka BRD1) are a group of paralogs found within HAT complexes which have been predicted play a critical role in acute myeloid leukemia.[61,62] This improved understanding of BRPF1/2/3 and the relatively advanced target validation of their bromodomains is reflected in the sophisticated portfolio of effective chemical probes available.

At the time of our previous review, the BRPF1/2/3 chemical probe tool box was already well established with several potent inhibitors (pK_D = 7-8) being disclosed, typically bearing a dimethyl imidazolidinone scaffold. Since then a multitude of additional BRPF1/2/3 inhibitors have been published, again built around the same dimethyl imidazolidinone scaffold which continues to dominate the BRPF1/2/3 chemical probe landscape. Despite little to no advances in potency and diversity, the selectivity of BRPF1/2/3 inhibitors has improved, selectivity over the BET subfamily, but also within the BRPF paralogs.

One of the more recent additions to the BRPF1/2/3 chemical probe tool box is GSK6853 (**44**), a potent and highly selective BRPF1 bromodomain inhibitor optimized from the previously reported BRPF1 inhibitor GSK5959 (**43**).[63] In optimizing **43** to **44**, GSK improved the solubility from 8 µg/mL to 140 µg/mL, and consequently improved its applicability to *in vivo* experiments.[64,65] This was achieved through the introduction of a basic nitrogen at the 6-position of the piperidine ring, improving the compounds physicochemical properties whilst in turn forming a hydrogen bond to Asn651 carbonyl to maintain potency, as predicted by X-ray crystallography (**Figure 9e**). Further interrogation of the crystal structure presented the 2-position of the piperidine ring as a vector towards Pro658, one of only a few residues not conserved between the BRPF family, where a favourable interaction with a methyl group was harnessed for improved BRPF1 potency (pIC_{50} = 8.1) and BRPF sub family selectivity (BRPF2 = ×1000 and BRPF3 >×1000). Moreover, **44** retained its high selectivity over BET bromodomains (>×1600) as measured by TR-FRET assay and was selective (>×2000) against a further 26 non-BET bromodomains in the DiscoverX BROMOscan panel. Additionally, **44** displayed selectivity (×500) against a cross screen panel of 48 pharmacologically relevant off targets including kinases, ion channels, GPCRs, enzymes, transporters and a nuclear receptor. The cellular activity of **44** was then demonstrated using a NanoBRET assay where potent inhibition (BRPF1 pIC_{50} = 7.7) was displayed. Along with GSK9311 (**45**), a structurally related negative control, **44** shows good potential for use as a chemical probe of BRPF1. Furthermore, **44** also possesses suitable PK for *in vivo* mouse studies following intraperitoneal delivery.

Collaborative work between Bayer and the SGC has led to the identification of BAY-299 (**47**), a potent and selective triple inhibitor of BRPF2 (BRPF2 pIC_{50} = 7.2) and TAF1/TAF1L (TAF1 pIC_{50} = 8.1).[66] An initial HTS of ~3.5 million compounds resulted in potent (BRPF2 pIC_{50} = 6.3) hit compound **46**, selected for displaying selectivity over BRD4 (BRD4(1) pIC_{50} = 4.9). Optimization of potency, solubility, *in vitro* DMPK and selectivity

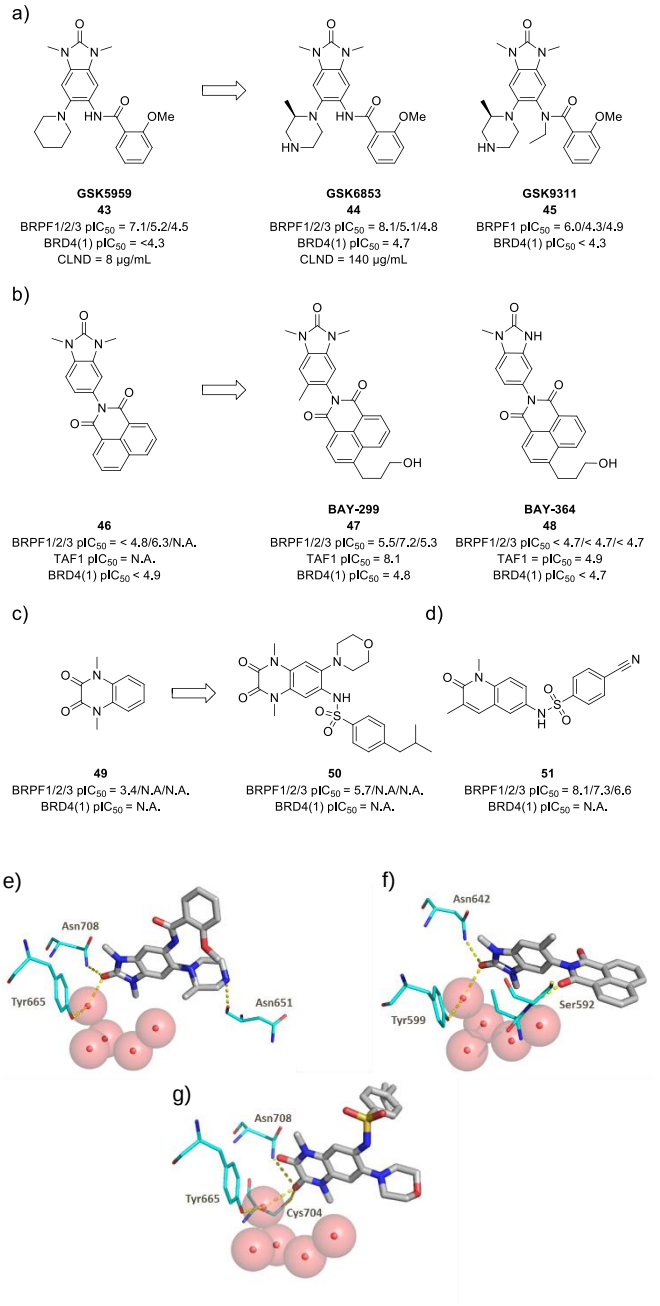

Figure 9. a) Structure of BRPF1 chemical probe **44**, accompanying negative control **45**, and starting point **43**; b) Structure of BRPF1/TAF1 dual inhibitor **47**, accompanying negative control **48**, and hit compound **46**; c) Structure of BRPF1 inhibitor **50** and initial hit compound **49**; d) Reference patent BRPF1 inhibitor **51**; e) Crystal structure (PDB: 5G4R) of **44** (grey) bound to human bromodomain BRPF1 (cyan); f) Crystal structure (PDB: 5N49) of **44** (grey) bound to human bromodomain BRPF2 (cyan); g) Crystal structure (PDB:5MWH) of **50** (grey) bound to human bromodomain BRPF1 (cyan).

resulted in **47**, with a key interaction between a carbonyl group and Ser592 providing the desired BRPF2 selectivity (**Figure 9f**). **47** was shown to engage BRPF2 (BRPF2 pIC_{50} = 7.2) selectively over BRPF1 (BRPF1 pIC_{50} = 5.5) and BRPF3 (BRPF3 pIC_{50} = 5.3) as measured by a TR-FRET assay. **47** also demonstrated selectivity over the BET subfamily (BRD4 pIC_{50} = 4.8), >300 kinases (<50% inhibition in all cases at 10 µM) and against a LeadProfilingScreen containing 68 pharmacologically relevant

targets (<25% inhibition in all cases at 10 μM). Selectivity was also demonstrated against 32 bromodomains in an alpha screen assay excluding CREBBP where at 100 nM modest CREBBP potency was shown (CREBBP pIC_{50} = 5.8). **47** demonstrated permeability (Caco2 cell P_{app} = 163 nm/s) and was shown to successfully engage BRPF2 (pIC_{50} = 6.3) and TAF1(2) (pIC_{50} = 6.0) within cells, as measured by NanoBRET assay, despite poor solubility (10 μg/mL). A structurally similar negative control, BAY-364 (**48**), was also developed and showed reduced potency at both BRPF2 (BRPF2 pIC_{50} <4.7) and TAF1 (TAF1 pIC_{50} = 4.9). The polypharmacology of **47**, however, hinders assigning any observed phenotype to a particular bromodomain. Bayer have subsequently published a patent disclosing a number of other BRPF1/TAF1 dual inhibitors based around the same dimethylated imidazolidinone core scaffold.[67]

In a deliberate attempt to expand the variety of chemotypes involved in BRPF1 inhibitors, Caflisch and co-workers developed **50**.[68] An initial fragment based pharmacophore search identified hit compound **49**. Molecular docking and a subsequent substructure search around the 1,4-dimethylquinoxaline-2,3-dione scaffold ultimately led to **50**. X-ray crystallography was used to identify key hydrogen bond interactions to the conserved Asn (Asn708), Cys704, and a water mediated hydrogen bond interaction to the conserved Tyr (Tyr665) (**Figure 9g**). Additionally, the phenyl ring of **50** was shown to form an edge-to-face π-π interaction to Phe714, the gatekeeper residue found in BRPF1's bromodomain, whilst the morpholine group forms a water mediated hydrogen bond to Gly650. **50** displayed potency at BRPF1 in Alpha screen (pIC_{50} = 5.7) and BROMOscan assays (pK_D = 5.7). 'Negligible activity' against the BET subfamily (BRD4), BRPF2/3, ATAD2 and CREBBP is reported for **50**, although no data is provided. Alternatively, activity against BRD9 is reported (BRD9 pIC_{50} = 3.7). No cellular activity data is reported for **50** and a negative control is not provided. **50** would benefit from further selectivity characterization, in particular against other non-BET bromodomains and pharmacologically relevant off targets, however does offer another BRPF1 inhibitor pharmacophore.

A patent released by UCL business PLC discloses a range of BRPF1 inhibitors based around a quinolinone scaffold.[69] A representative example, **51**, which displays potency for BRPF1 (pK_D = 8.1) is shown. Due to the nature of patents little extra data is provided, although potency against BRPF2 (pK_D = 7.3), BRPF3 (pK_D = 6.6), BRD7 (pK_D = 7.1) and BRD9 (pK_D = 6.5) is disclosed.

In combination with previously reported BRPF1/2/3 probes, **44**, and **47** help to expand the repertoire of BRPF1/2/3 chemical tools for target validation. Moreover, **47** offers promise for BRPF2 isoform selectivity, which along with BRPF3, remains an opportunity for probe development. Additionally, **50** provides hope for the development of BRPF1 inhibitors of varying chemotypes to help diversify the BRPF1/2/3 chemical tool repertoire, currently dominated by the dimethylated imidazolidinone scaffold.

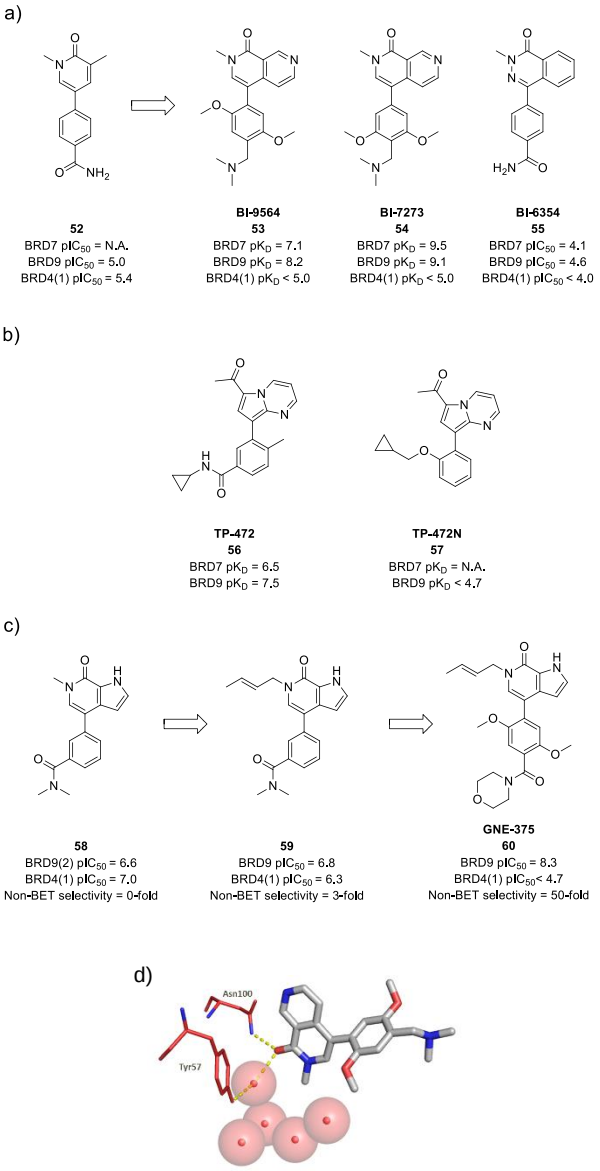

Figure 10. a) Structure of BRD7/9 chemical probe **53** and **54**, accompanying negative control **55** and initial hit compound **52**; b) Structure of BRD7/9 chemical probe **56** and accompanying negative control **57**; c) Structure of BRD7/9 chemical probe **60**, intermediate **59** and starting point **58**; d) Crystal structure (PDB: 5F1H) of **53** (grey) bound to human bromodomain BRD9 (red).

BRD7/9

Two BCPs with a repertoire of existing chemical probes are BRD7 and BRD9. BRD7/9 have both been implicated in the chromatin remodelling SWI/SNF complex and the PBAF/BAF complexes in humans respectively, each involved in the regulation of gene expression, making them promising targets for anti-cancer agents.[70] More specifically, BRD7 has been shown to function as a tumour suppressor across various cancers,[71–73] whilst BRD9 has been found to be involved in cancers through mutation or overexpression.[74]

At the end of 2015, the BRD7/9 chemical probe repertoire was already well developed including multiple dual BRD7/9 inhibitors and BRD9 selective inhibitors. In contrast, there were no disclosed BRD7 selective inhibitors or promise for future

development. Since then, a variety of new BRD7/9 inhibitors have been developed expanding the already diverse library. Additionally, a new chemical tool for BRD9 has been developed in the form of the first BRD9 PROTAC.

Collaborative work between the SGC and Boehringer Ingelheim has led to the development of BI-9564 (**53**), an *in vivo* capable potent and selective probe for both BRD7 and BRD9.[75] A fragment based screening approach utilizing a DSF assay to identify initial hits, such as **52**, was followed by structure guided design, leading to dual BRD7/9 inhibitors **53** and **54** (**Figure 10a** & **d**). **53** displayed potency for BRD9 (pK_D = 8.2) and BRD7 (pK_D = 7.1), and selectivity over the BET subfamily (BRD4(1) pK_D <5.0), as measured by a DiscoverX BROMOscan assay. With the exception of CECR2 (pK_D = 7.1), **53** was also shown to be selective against the remaining non-BET bromodomains showing no activity at the concentrations tested by ITC. The cellular activity of **53** was demonstrated at 1 µM in a FRAP assay using a green fluorescent protein-BRD9 fusion protein expressed in U2OS cells. **53** was also screened against 55 GPCRs and 324 kinases with only 2 GPCRs and 3 kinases showing >40% crtl inhibition at 10 µM. Additionally, **53**'s ability to function as an *in vivo* tool is supported by aqueous solubility (>90 µg/mL) and permeability (Caco2 P_{app} = 110 nm/s), and suitable PK within a mouse model following intravenous delivery. Likewise, **54** displayed subnanomolar potencies for BRD7 (pK_D = 9.5) and BRD9 (pK_D = 9.1) with selectivity over the BET subfamily (BRD4(1) pK_D < 4.7) as demonstrated by DiscoverX BROMOscan assay. Again, **54** appeared selective against the remaining non-BET bromodomains (>30-fold) with potency also observed for CECR2 (pK_D = 8.1). **54** was also shown to engage both BRD7/9 with 100% inhibition at 1 µM in FRAP assays, demonstrating target engagement and cellular permeability (Caco2 P_{app} = 14 nm/s), and is accompanied by suitable PK parameters within a mouse model following intravenous delivery. Finally, **53** and **54** are accompanied by negative control BI-6354 (**55**), although the structural differences should be acknowledged.[76]

TP-472 (**56**), another potent and selective BRD7/9 probe, has recently been developed by the SGC and Takeda with a novel BRD7/9 binding chemotype (**Figure 10b**). **56** reports good potency for BRD7 (BRD7 pK_D = 6.5) and BRD9 (BRD9 pK_D = 7.5) and >×30 selectivity over the remaining bromodomains. Although no solubility or permeability data is supplied, **56** cellular activity was demonstrated (BRD9 pEC_{50} = 6.5) in a BRD9 NanoBRET assay. A negative control, TP-472N (**57**), is also reported as being inactive against BRD9 at 20 µM, although the large structural differences should be considered. No data on the selectivity of **56** against other pharmacological off-targets is provided.[77]

Starting from the *N*-methyl pyrrolopyridone **58**, Crawford and co-workers substituted the *N*-methyl group for a selection of small hydrophobic substituents (**Figure 10c**). The introduction of hydrophobic substituents was shown to induce a narrow hydrophobic channel in the binding pocket of BRD9.[78] Substitution of the N-Methyl group for a crotyl group (**59**) reduced the potency for BRD4, BRPF1, CECR2, CREBBP and TAF1,

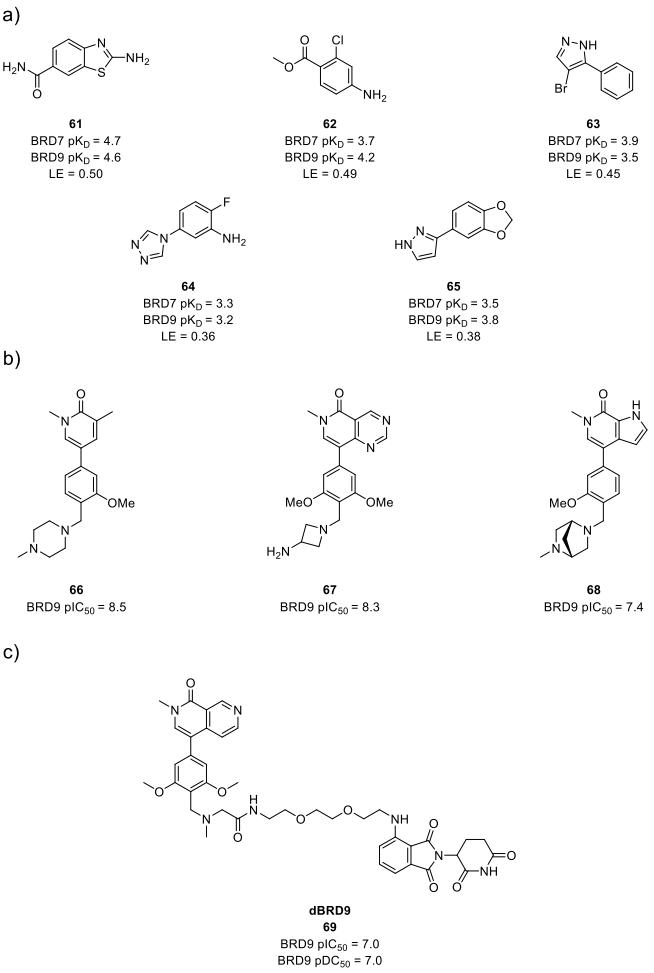

Figure 11. a) Structures of BRD7/9 fragments **61**-**65**; b) Structure of reference patented BRD7/9 inhibitors **66**-**68**; c) Structure of BRD7/9 PROTAC **69**;

whilst maintaining submicromolar potency for BRD9 (pIC_{50} = 6.8). Although potency at BRD4 (pIC_{50} = 6.3) was reduced, only moderate selectivity was observed. **59** was then subject to lead optimization efforts, focussing primarily on occupying accessible space in the ZA channel through para substitution of the benzene ring. Additionally, substitution off the ortho and meta positions of the benzene ring was hypothesised to occupy a small pocket in BRD9, further enhancing selectivity, eventually leading to GNE-375 (**60**).[79] **60** exhibited potency at BRD9 (pIC_{50} = 8.3) and >3000-fold selectivity over the BET bromodomains (BRD4(1) pIC_{50} = <4.7) as measured by TR-FRET assays. Potency (BRD9 pK_D =

8.7) and selectivity against other non-BET bromodomains was also confirmed using a BROMOscan panel with >1500-fold selectivity observed against the panel, excluding the highly homologous BRD7 (pK_D = 7.0) where 50-fold selectivity was observed. **60** was also screened against an Invitrogen 40 kinase panel where no inhibition >20% was observed at 1 μM, and a CEREP panel where activity was observed against a GABBA receptor (86% at 10 μM). **60** demonstrated target engagement in a cellular thermal shift assay (44-50 °C), albeit at 2 μM. After demonstrating cellular viability, **60** was then used in the target validation of BRD9 bromodomain inhibition. RNA sequencing analysis of gene expression following a 24-hour treatment with **60** showed inhibition of 7 genes. Of note was the inhibition of ALDH1A1, an enzyme whose levels and activity have been shown to be increased in crizotinib resistant gastric cancer lines.[80] ALDH1A1 and its promoter are regulated by acetylation, suggesting BRD9 could play an active role in either/both of these mechanisms and proposes a new area for therapeutic intervention strategies.

NMR fragment-based screening has been used to discover five ligand efficient fragments (**61**-**65**) for future BRD7/9 inhibitor optimization (**Figure 11a**). Of particular interest is bromo pyrazole fragment **62** which appears to show ×2.5 selectivity for BRD7 over BRD9 and potential for the development of selective BRD7 bromodomain inhibitors.[81]

Numerous patents disclosing BRD7/9 inhibitors have also been published since the last review. Following on from their work developing BRD7/9 chemical probes, Genentech and Constellation Pharmaceuticals have disclosed five additional BRD7/9 inhibitors based around the pyrolopyridinone scaffold discussed above.[82] BRD9 potency (pIC_{50} = 7.4) and selectivity data is reported (200-fold selectivity over the BET subfamily of bromodomains and 400-fold selectivity over 7 representative non-BET bromodomains) for one compound, although the structure is not specified. Due to the nature of patents no further data is provided.

Similarly, Boehringer Ingelheim have released a patent disclosing numerous BRD9 inhibitors spanning three different, albeit related, chemotypes. Cellular activity data in either a BRD9 H3 or BRD9 H4 assay is provided, and the most potent of each chemotype **66** (BRD9 pIC_{50} = 8.5), **67** (BRD9 pIC_{50} = 8.3) and atropisomer **68** (BRD9 pIC_{50} = 7.4) are included for reference. All three chemotypes show potency for BRD9 and cellular target engagement, however no further characterization is provided.[83]

Bradner and co-workers have disclosed dBRD9 (**69**) the first BRD9 PROTAC.[84] A selection of BRD9 PROTACs were synthesised based around three different BRD9 chemical probes, LP99, I-BRD9, both of which were reviewed previously,[13] and **54** discussed above. **54** was eventually chosen to function as the selective BRD9 inhibitor part of the PROTAC, due to improved BRD9 selectivity (in particular selectivity over the BET subfamily) when compared to LP99 and I-BRD9 PROTAC derivatives, highlighting the advances that have been made in BRD9 chemical probe development since our last review. To complete the bifunctional PROTAC, an E3 ligase recruiter (a pomalidomide conjugate) was appended via a poly-ethylene glycol (PEG) to produce **69**. **69** maintained potency for BRD9 (pIC_{50} = 7.0) and selectivity over the BET subfamily (BRD4(1) pIC_{50} < 4.3). BRD9 was selectively degraded over a range of potencies using **69** (BRD9 pDC_{50} = 7.0). The cellular selectivity of **69** was then demonstrated using MOLM-13 cells, in which, out of the 7326 proteins quantified, only BRD9 showed a statistically significant difference in abundance (5.5-fold decrease after treatment with 100 nM of **67** for 2 hours). A control species for **69** was generated through the removal of the acetylated lysine mimetic, thus removing any potency for BRD9 (pIC_{50} < 5). Interestingly, both **69** and its inactive negative control retained activity against the IKZF family of transcription factors and should be accounted for when using **69** for target validation. The development of non-BET bromodomain PROTACs will help expand the target validation of these proteins into the effects of degradation in comparison to bromodomain inhibition.

The discussed BRD7/9 inhibitors help expand the BRD7/9 chemical tool repertoire, both in quantity and diversity, although there still appears to be a reliance on bi-aryl scaffolds in the pursuit of selective BRD7/9 probes. Along with the existing BRD7/9 selective chemical probes, and introduction of a new BRD9 degrader, target validation for the bromodomains of BRD7/9 and dissection of the individual roles of each proteins bromodomains, shows promise, one omission being the absence of a selective BRD7 probe.

ATAD2/ATAD2B

ATAD2 and ATAD2B are chromatin remodelling proteins which consist of an AAA^+ ATPase domain and a highly homologous (76% consistent amino acid sequence) bromodomain. Both proteins have been strongly linked with a diverse range of cancers including lung,[85] liver,[86] prostate and breast, hence the desire for ATAD2/ATAD2B chemical probes for further target validation.[87, 88] At the end of 2015, the ATAD2/ATAD2B chemical repertoire was in its infancy, with one optimized ATAD2/ATAD2B inhibitor disclosed, which unfortunately showed activity against TAF1/TAF1L. Since then, the ATAD2/ATAD2B chemical tools available have grown, with the first ATAD2/ATAD2B chemical probe, and ATAD2 isoform selective chemical probe being developed.

GSK have reported ATAD2 chemical probe, GSK8814 (**72**), optimized from their previously reported ATAD2 inhibitor (**71**) (**Figure 12a**).[89] Of note was the substitution of the sulfone group for the more polar $-CF_2$ bioisostere which provided a needed increase in permeability, along with an increase in solubility. Secondly, 1,3-interactions on the piperidine ring were utilized to destabilise the axial conformation favoured for BRD4(1) binding, thus improving selectivity over the BET subfamily (**Figure 12d**). **69** demonstrated potency for ATAD2/2B (ATAD2/2B pIC_{50} = 7.3/7.7) with selectivity over the BET family (>×1000) and other non-BET bromodomains (×100). Cellular target engagement of **66** with ATAD2 (pIC_{50} = 5.7) was demonstrated using a NanoBRET assay and was reflected in the solubility (2313 μg/mL) and permeability (190 nm/s) of **72**. Moreover, **72** was screened against an internal GSK panel of 40 pharmacological off-targets and was inactive at the concentrations tested. The corresponding enantiomer of **69**, known as GSK8815 (**73**), displayed a reduced potency for ATAD2/2B (pIC_{50} = 5.5/5.5) and provides an enantiomeric negative control for phenotypic screening.[90]

An alternative conformation locking strategy for disfavouring BRD4(1) binding has also been reported by GSK utilizing a tropane group in place of the piperidine ring.[91] As discussed above, forcing the polar shelf group into an equatorial position, as seen with tropolone derivatives, strongly favours ATAD2 (pIC_{50} = 6.6) binding over BRD4(1) (pIC_{50} < 4.3) resulting in an improved

selectivity (>250-fold). As a result, **74** provides further evidence to support the development of BET selective ATAD2 chemical probes through conformational locking.

Bayer have recently reported BAY-850 (**76**), the first ATAD2 isoform selective inhibitor. An initial screening of 11 DNA encoding chemical libraries, amounting to ~65 billion compounds, resulted in hit molecule **75**.[92] The two stereogenic centres were quickly identified as crucial for ATAD2 potency and optimization was focussed primarily on the methyl amide, with substitution for a more lipophilic and basic cyclohexyl diamine providing the required potency boost. **76** showed good potency for ATAD2 (pK_D = 6.9) and selectivity against a wide range of other BET and non-BET bromodomains (31 DiscoverX BROMOscan panel), with only BRD3(1) and BAZ2B showing greater than 50% inhibition at 10 µM. Similarly, **76** appeared selective against a panel of 354 kinases and 25 GPCRs with only modest potency shown for a few GPCRs. Solubility (>3070 µg/mL) and permeability (39 nm/s) were also reported for **76** which, as a result, successfully demonstrated cellular activity at 1 µM via a FRAP assay as evidence of target engagement. Uniquely amongst published ATAD2 inhibitors, **76** appears selective over ATAD2B, suggesting a different mode of binding to that of the previously discussed ATAD2 inhibitors. Through the use of mass spectrometry and size exclusion chromatography, Bayer identified that **76** simultaneously binds two ATAD2 molecules to form a dimer complex. Moreover, **76** was accompanied by structurally related negative control BAY-460 (**77**), which together function as unique ATAD2 inhibitors for target validation.

Finally, Miller and co-workers have reported **79** as a novel ligand for ATAD2 inhibitor development (**Figure 12c**). Initial hit fragment **78** was identified via crystallographic fragment

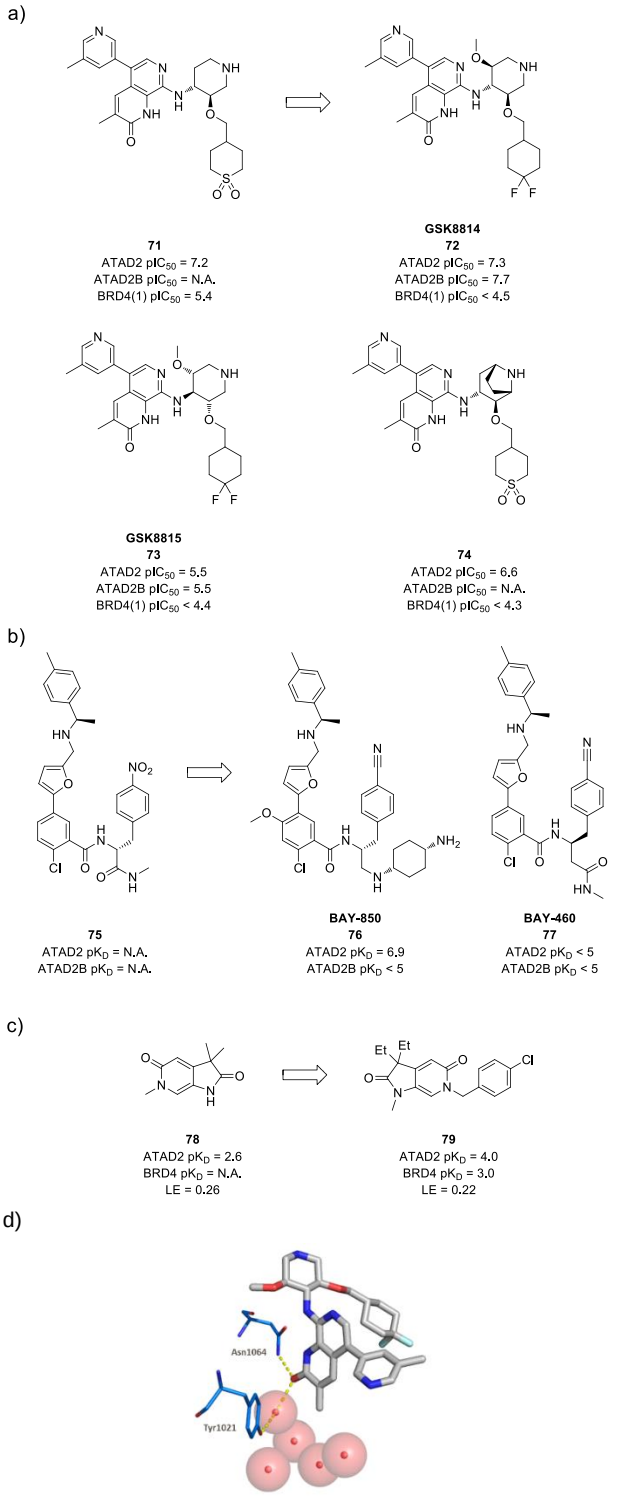

Figure 12. a) Structure of ATAD2/ATAD2B chemical probe **72**, accompanying negative control **73**, starting point **71** and additional inhibitor **74**; b) Structure of ATAD2 chemical probe **76**, accompanying negative control **77** and initial hit compound **75**; c) Structure ATAD2/ATAD2B inhibitor **79** and initial hit compound **78**; d) Crystal structure (PDB: 5LJ0) of **72** (grey) bound to human bromodomain ATAD2 (blue).

screening as a weak ATAD2 inhibitor. Interestingly, methylation of the pyrrolodinone lactam resulted in a change in binding mode to ATAD2, with the pyrrolodinone lactam functioning as the

acetylated lysine mimetic. Further structure guided optimization resulted in **79** which showed weak potency for ATAD2 (pK_D = 4.0) and 10-fold selectivity over the BET subfamily. **79** offers potential for future ATAD2 inhibitor development following further optimization.[93]

76 and **79** provide new inhibitors and chemotypes for future ATAD2 chemical probes. Additionally, **72** expands on an existing chemotype to deliver a high quality ATAD2 chemical probe. When combined with the existing array of ATAD2 inhibitors target validation of ATAD2's bromodomains looks promising. Additionally, the promise of achieving isoform selective ATAD2/ATAD2B inhibitors bodes well for dissecting their individual roles in disease.

TRIM24

Tripartite motif-containing 24 (TRIM24) is a transcription coregulator whose over expression has been correlated to a wealth of different cancers.[94–96] Our previous review concluded with the disclosure of two dimethylated imidazolidinone TRIM24 inhibitors, both of which reported activity at the BRPF subfamily of bromodomains. Since then, it has been shown that inhibition of TRIM24's bromodomain fails to exert an effective anti-proliferative response, thus suggesting that bromodomain inhibition alone is insufficient for anti-cancer therapeutic development.[97] As a result, no further TRIM24 inhibitors have been disclosed for use as chemical probes, instead work has begun into the development of more sophisticated TRIM24 chemical tools.

Bradner and co-workers disclosed dTRIM24 (**81**), the first TRIM24 PROTAC and degrader (**Figure 13a**).[98] Starting from a derivative of previously reported TRIM24 chemical probe IACS-9571 (**80**), a VHL E3 ligase inhibitor was appended via a PEG linker to create bifunctional molecule **81**. Bifunctional molecule **81** displayed similar potency to TRIM24 inhibitor **80**. Likewise, a similar selectivity profile was observed for **81** against a panel of 32 bromodomains, with equipotency shown against BRPF1 and BRPF2. Cellular permeability was also demonstrated via a VHL degron displacement assay, providing evidence of target engagement. Importantly, **81** was shown to solely degrade TRIM24 (despite selectivity concerns with BRPF1/2) substantially at 4 hours and degradation was maintained over 72 hours. Whereas TRIM24 inhibitors have been shown to display no anti-proliferative phenotype in the treatment of leukaemia, tumours of hematopoietic origin were sensitive to degradation of TRIM24, highlighting TRIM24 as a novel target for acute leukaemia therapeutics.

Introduction of a TRIM24 PROTAC to the TRIM24 chemical tool repertoire offers a unique form of target validation through TRIM24 degradation. **81** also demonstrates that partially selective inhibitors can produce selective degraders yet highlights the importance for high quality chemical probes in the development of more sophisticated tools.

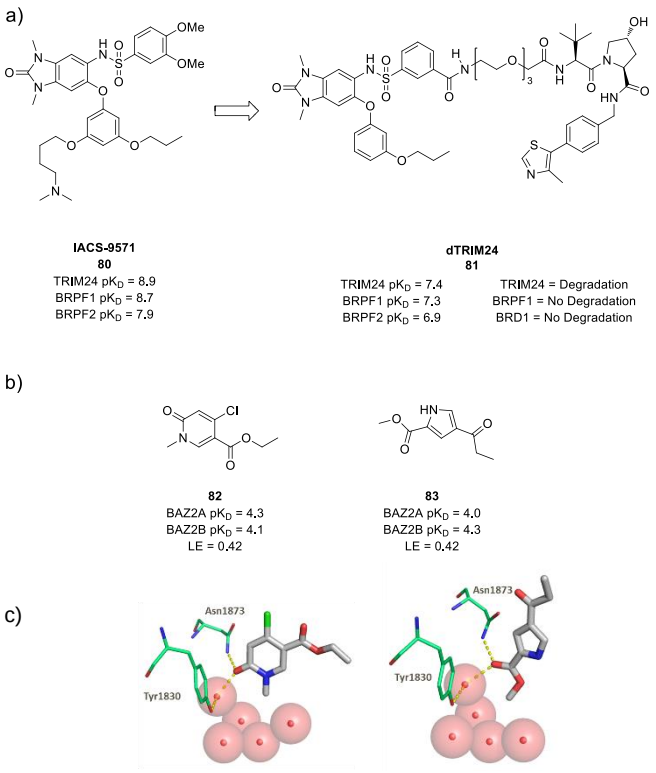

Figure 13. a) Structure of TRIM24 PROTAC **81** and starting point **80**; b) Structure of BAZ2A/BAZ2B fragments **82** and **83**; c) Crystal structures (PDB: 5MGJ and 5MGK) of **82** (grey) and **83** (grey) bound to human bromodomain BAZ2A (green).

BAZ2A/BAZ2B

Bromodomain Adjacent to Zinc finger domain 2A/B (BAZ2A/B) are essential components of the chromatin remodelling complex NoRC (Nucleolar remodelling complex) and are implicated in the cell growth and disease recurrence of prostate cancer.[99]

At the time of our previous review, the BAZ2A/BAZ2B landscape contained multiple diverse BAZ2A/BAZ2B inhibitors. Since then, additional fragment inhibitors have been developed which offer promise for further BAZ2A/BAZ2B chemical probe development and diversification.

Spiliotopoulos and co-workers have recently reported the discovery of two ligand efficient (LE >0.4) BAZ2A/BAZ2B inhibitors **82** and **83**.[100] *In silico* docking of 1413 small molecules into the acetylated lysine binding site of BAZ2A was used to identify an initial 20 small molecule fragment library which were then validated by ligand based NMR spectroscopy. 7 of the initial 20 small molecules showed specific interactions with BAZ2A, which were then, in turn, evaluated in an *in vitro* competitive binding assay based on DNA-tagged BAZ2A bromodomain and polymerase chain reaction (PCR) quantification. X-ray crystallography was then used to compare the binding modes for **82** and **83**. As predicted by *in silico* docking, the aromatic rings of both **82** and **83** were shown to be sandwiched between the hydrophobic sidechains of the gate keeper residue (Val1879) and two other Val residues (Val1822 and Val1827), whilst the methyl lactam of **82** and the ethyl ketone of **83** were shown to act as the acetylated lysine mimetics (**Figure 13c**). Additionally, van der Waals interactions were observed between the 4-chloro and 3-

ethyl-ester substituents of **82** and the side chains of Val1827 and Trp1816-Pro1817 respectively, whilst a weak polar interaction between the aromatic CH at position 2 and the carbonyl of Pro1817 was also observed. Optimization to install the required selectivity and physicochemical properties has been proposed through two growth pathways: 1) towards Glu1820/Leu1891 and 2) towards Ser1828/Pro1899.

Although **82** (BAZ2A/BAZ2B pK_D = 4.3/4.1) and **83** (BAZ2A/BAZ2B pK_D = 4.0/4.3) are not potent enough to be considered BAZ2A/BAZ2B inhibitors or chemical probes, they do offer two novel ligand efficient chemotypes for the development of future BAZ2A/BAZ2B chemical probes to add to the existing BAZ2A/BAZ2B chemical probe tool box.

TAF1/TAF1L

TAF1 and TAF1L are associated factors of the TATA binding protein (TBP), a large subunit of transcription factor II D (TFIID) and are believed to help facilitate the binding of TBP to DNA promoter regions and to add promoter selectivity. Like many BCPs, TAF1/TAF1L are believed to be associated with a number of oncology diseases, including cervical cancer,[101] prostate cancer,[102] and colorectal and gastric cancers[103]. Additionally, TAF1/TAF1L have been strongly linked to neurodegenerative diseases such as intellectual disability[104] and X-linked dystonia parkinsonism.[105] TAF1 and TAF1L both possess tandem bromodomains, with high homology shown across both bromodomains and the proteins in general (95% amino acid sequence). As a result, it is likely that compounds that bind TAF1 will also bind TAF1L. Consequently, data is typically reported for TAF1(2) with almost no data reported for TAF1(1), TAF1L(1) or TAF1L(2).

Only one TAF1/TAF1L inhibitor (TAF1(2) pK_D = 6.3), which showed a higher potency for the BET bromodomains, was disclosed at the time of our last review. Since then, the TAF1/TAF1L chemical tool repertoire has advanced dramatically in number, with multiple inhibitors being developed with improved potency (pK_D > 7.0) and BET selectivity. Unfortunately, selectivity over other non-BET bromodomains has proven tricky, with several of the reported inhibitors displaying potency for other bromodomains.

Whilst investigating BRD4 inhibition Sdelci and co-workers discovered a selection of small molecules that mimic BRD4 inhibition, without binding to the target. One of these small molecules, CeMMEC13 (**84**), was shown to inhibit TAF1(2) (pIC_{50} = 5.7) with selectivity against the BET subfamily (<20% inhibition against BRD4 at 10 µM). **84** also displayed selectivity over other non-BET bromodomains tested (<60% inhibition against BRD9, CREBBP and EP300 at 10 µM). In addition, **84** was also shown to engage TAF1(2) within REDS3 cells, confirming its cellular activity. CeMMEC15 (**85**) was also developed as a negative control, although the two compounds are structurally quite different. In addition compound **84** would benefit from further selectivity

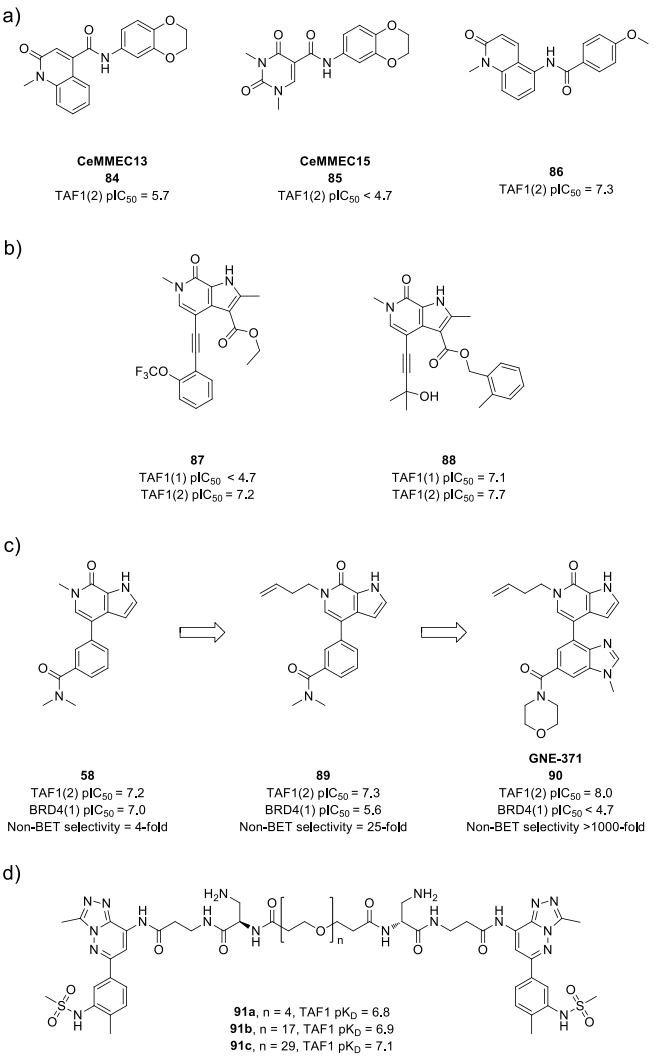

Figure 14. a) Structure of TAF1/TAF1L inhibitor **84** and accompanying negative control **85**, and reference patent compound **86**; b) Structures of reference patent TAF1(2) selective inhibitor **87** and panTAF1 inhibitor **88**; c) Structures of TAF1 inhibitor **90**, intermediate **89** and starting compound **58**; d) Structure of bivalent TAF1 inhibitors **91a-c**;.

characterization, in particular against the remaining non-BET bromodomains.[106] Continuation of this research has lead the Research Center for Molecular Medicine to release a patent disclosing further TAF1 inhibitors.[107] Although limited data is provided for the molecules, the most potent inhibitor (TAF1(2) pIC_{50} = 7.3) has been included for reference (**86**), and shows an increase in potency from **84**.

A series of TAF1 inhibitors have also been discovered by collaborative work between Genentech and Constellation pharmaceuticals and disclosed in a recent patent.[108] 208 compounds were synthesized and tested for potency against both bromodomains of TAF1. Two compounds, the most selective TAF1(2) compound (**87**) and the most potent panTAF1 compound (**88**) have been included for reference. **87** displayed potency for TAF1(2) (pIC_{50} = 7.2) and was selective over TAF1(1) (pIC_{50} <4.7). By contrast, compound **88** displayed potency towards both

bromodomains of TAF1 (BD1/BD2 pIC_{50} = 7.1/7.7). It is currently unknown whether selective TAF1(2) inhibition or panTAF1 inhibition is preferred, however, having access to inhibitors of each type will help elucidate this information. As to be expected for compounds disclosed in a patent, no information on selectivity, solubility, permeability or cellular target engagement has been disclosed.

As discussed in the BRD7/9 section, Genentech and Constellation pharmaceuticals have reported selective bromodomain inhibitors where selectivity can be attributed to bromodomain specific interactions with the conserved water network found within the bromodomain binding pocket.[78] Substitution of the *N*-methyl group of hit molecule **58** for a 1-butene group (**89**) dramatically reduced the potency for BRD4, BRD9, BRPF1, CREBBP and CECR2, whilst maintaining submicromolar potency for TAF1(2) (pIC_{50} =7.3). **89** was subjected to iterative structure-based drug design leading to **90**.[109] Introduction of a morpholine group to the benzamide provided an optimal occupancy of the lipophilic-shelf region and an accompanying boost in TAF1(2) potency. Additionally, substitution off the phenyl ring was utilized to induce disfavourable protein surface interactions within BRD4(1), thus reducing BRD4(1) potency and improving BET selectivity. **90** displayed potency for TAF1(2) via TR-FRET (pIC_{50} = 8.0) and BROMOscan (pIC_{50} = 9.0) assays, and selectivity over the BET family (×2000). Furthermore, **90** was screened against 37 additional bromodomains via the BROMOscan panel where ≥1000-fold selectivity was observed excluding TAF1L(2) where equipotency was observed. Similarly, **90** appeared selective against a 35-kinase panel (<17% inhibition observed at 1 µM). Finally, cellular target engagement was demonstrated using a NanoBRET assay where submicromolar potency (pIC_{50} = 7.4) was observed.

Exploiting the tandem nature of the bromodomains in TAF1, Frye and co-workers have reported the first examples of bivalent TAF1 inhibitors.[110] Starting from the bromosporine derived ligand UNC4993, three bivalent TAF1 inhibitors were developed, each containing two UNC4993 monomers connected via polyethylene glycol (PEG) linkers. The most potent bivalent inhibitor, **91c**, was shown to have a marginally enhanced potency (TAF1 pK_D = 7.1) compared to the monovalent inhibitor (TAF1 pK_D = 6.7), possibly attributable to the bivalent nature of the inhibitor. The bromodomain promiscuity of bromosporine ligands raises doubt over the selectivity of the inhibitors, in particular over the dual bromodomain BET subfamily, although theoretically this could be controlled by the linker length. Unfortunately, no selectivity data for the inhibitors is reported, nor for the monovalent inhibitor UNC4993. Additionally, no permeability or solubility data is provided, or evidence of target engagement. Absence of the above data highlights the caveats to using these bivalent inhibitors in target validation, however, further characterization could provide access to target validation of both TAF1 bromodomains.

Finally, as discussed previously, collaborative work between Bayer and the SGC has led to the identification of **47**, a potent and selective inhibitor for both BRPF1 (pIC_{50} = 8.2) and TAF1(2) (pIC_{50} = 7.9). For the same reasons discussed previously, caution should be taken when using **47** as a sole TAF1/TAF1L chemical probe.

Despite the growing number of diverse TAF1/TAF1L inhibitors, a lack of characterization, in particular regarding selectivity, suggests further TAF1/TAF1L inhibitor development is required to achieve adequate TAF1/TAF1L target validation. **90** does, however, show major progress towards reaching this goal. Additionally, dissecting the individual roles of TAF1/TAF1L's four bromodomains will also require further development into the possibility of non-pan TAF1/TAF1L inhibitors.

SMARCA2/4 & PB1

SMARCA2/4 and PB1 together make up the whole of sub family VIII and are all components of the mammalian SWI/SNF chromatin remodelling complex, where loss of function has been linked to several cancers.[111,112]

At the time of our previous review, the SMARCA2/4 bromodomains had undergone minor target (in)validation using the single SMARCA2/4/PB1 inhibitor available. Since then, additional SMARCA2/4/PB1 inhibitors have been developed with improved characterization, including inroads into selectivity within the subfamily.

Sutherell and co-workers have developed a collection of potent and selective SMARCA2/4/PB1 bromodomain inhibitors. Starting from a weakly potent, and poorly soluble, dihydropyrroloquinazolinone hit compound **92**, structure guided optimization led to lead compound **93**.[113] X-ray crystallography was used to identify the two key hydrogen bond interactions between the carbonyl group and nitrogen atom of the 4-quinazolinone scaffold, and the conserved Asn (Asn739) and Tyr (Tyr696). Similarly to previously reported SMARCA2/4/PB1(5) inhibitor PFI-3, **93** showed complete displacement of the conserved water molecules found within the binding pocket of SMARCA4. This distinctive binding action contrasts reported inhibitors of other bromodomains where the water molecules remain in place. A halogen bond between the chlorine atom and the carbonyl of a methionine residue (Met731) was also observed via X-ray crystallography (**Figure 15c**). Substitution of the chlorine for a bromine, in an attempt to create a stronger halogen bond, was countered by the steric constraint of the cavity. **93** demonstrated potency for PB1 (pK_D = 6.9), SMARCA2B (pK_D = 6.6) and SMARCA4 (pK_D = 6.4), and selectivity against a selection of other representative bromodomains (BRD4, PCAF, CREBBP, TRIM33B). A full selectivity profile against the remaining bromodomains was not provided, and similarly no data was provided on activity for pharmacologically relevant off-targets. Furthermore, no solubility or permeability data was reported for **93**, although "improved" physicochemical properties are reported, and cellular activity was demonstrated at 1 µM using a FRAP assay. Finally, no structurally related negative control was provided for **93**.

Also of note was the development of **94**, a biased PB1(5) inhibitor (ΔT_m = 10.2 ºC) with reduced SMARCA4 potency (ΔT_m = 2.9 ºC), as measured by DSF, the first inhibitor reported to do so. ITC was used to confirm potency for PB1(5) (pK_D = 6.8) and selectivity over SMARCA4 (pK_D = 5.7). It was hypothesized that the introduction of the ethyl groups occupied the ill-defined peptide-binding channel present in PB1(5), which is blocked in SMARCA4 by Ile543. Although no structure was obtained to confirm the blocking in SMARCA4, this does potentially present a new avenue to pursue in the development of selective PB1 chemical probes.

Additionally, a patent released by Genentech and Constellation Pharmaceuticals disclosed several SMARCA2/4 and PB1(5) inhibitors containing a pyridazine scaffold.[114]

SMARCA4 potency data was reported for each compound, the most potent of which **95**, has been included as reference. Potency against SMARCA2 and PB1(5) was also provided for select compounds and the most potent pan SMARCA2/4/PB1(5) triple inhibitor **96** has also been included.

Finally, a SMARCA2/4 small molecule inhibitor (**98**) has been developed by Luo and co-workers.[115] Starting from a HTS of 20,000 structurally diverse compounds, initial hit compound **97** was identified as a novel SMARCA2/4 inhibitor (pIC_{50} = 4.4). A subsequent 2D similarity based search revealed **98** as a more potent (pIC_{50} = 5.0) SMARCA2/4 inhibitor, and molecular docking was utilized to identify the key interactions between **98** and the SMARCA2 bromodomain. A similar binding mode to previously reported SMARCA2/4 inhibitor PFI-3 was identified along with the traditional hydrogen bond interaction between the amine and the conserved Asn (Asn1464). An additional hydrogen bond interaction between the pyridine nitrogen and a backbone Phe (Phe1409) residue was also observed (to which the boost in potency can be attributed) along with the expected water mediated hydrogen bond to the conserved Tyr (Tyr1421). Further insight into the selectivity of **98** would be beneficial, in particular over the BET subfamily, SMARCA4 and PB1, however **98** does offer a new chemotype start point for further optimization in the pursuit of SMARCA2/4 chemical probes.

Even with the addition of the above inhibitors, the SMARCA2/4/PB1(5) chemical tool pool remains shallow, with additional chemical probes required for all 3 BCPs for adequate target validation. In particular, improved selectivity between the bromodomains would allow for dissection of their individual pharmacology.

3. Atypical Non-BET Bromodomain Inhibitors

As eluded to in Section 1, atypical bromodomains do not possess the characteristic conserved Asn found throughout most bromodomains. Instead the Asn is mutated for a Tyr, Thr or Asp. As a result, the interactions we typically try to mimic with bromodomain inhibitors are different. Additionally, this causes a dramatic change to the depth of the atypical bromodomain binding pockets and overall increases the complexity of designing atypical

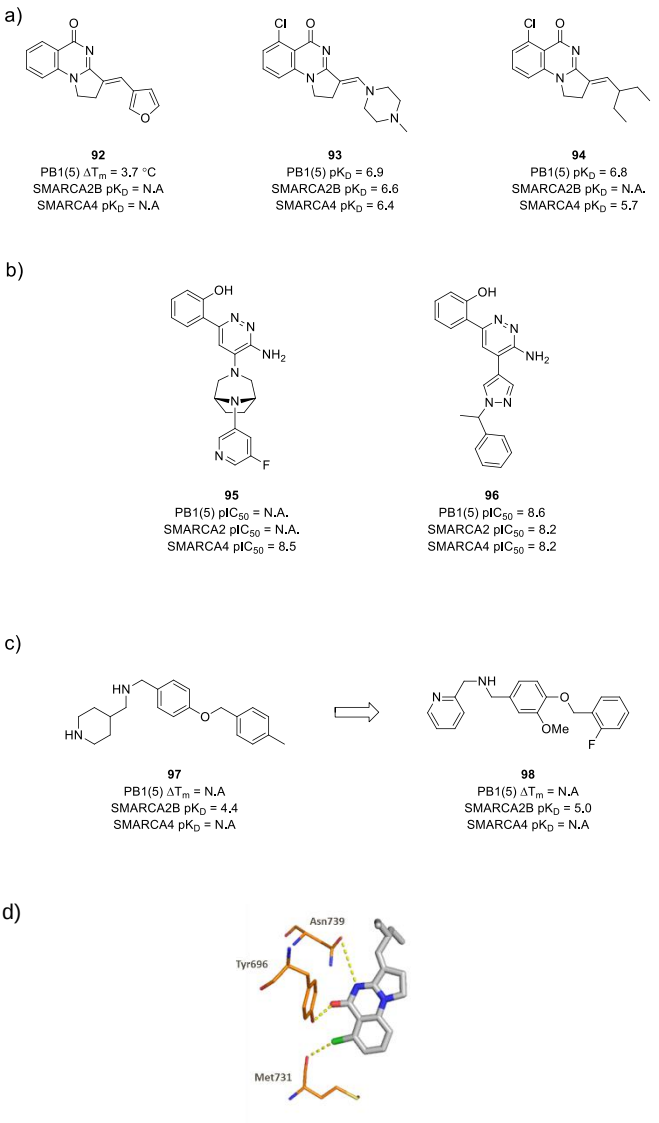

Figure 15. a) Structure of SMARCA2/4/PB1 inhibitors **92**-**94**; b) Structures of reference patent SMARCA2/4/PB1 inhibitors **95** and **96**; c) Structures of SMARCA inhibitor **98** and initial start point **97**; d) Crystal structure (PDB: 5FH8) of **94** (grey) bound to human bromodomain PB1(5) (orange) and the displaced water network.

bromodomain inhibitors. At the time of our first review there were no reported atypical bromodomain inhibitors. Similarly, since that review, little progress has been made to tackle this issue, with atypical bromodomain chemical probes remaining a challenge for the future.

PHIP

Pleckstrin homology domain interacting protein (PHIP) was originally identified through interactions with insulin receptor signalling proteins, yet has recently been reported as being involved in oncology.[116] More specifically PHIP has been identified as a promoter of melanoma metastasis and as a potential therapeutic target for breast and lung cancer, emphasising the need for further PHIP target validation.[117,118] The second bromodomain of PHIP is atypical, with a Thr present within the binding site instead of the typical Asn which has made

the development of PHIP(2) inhibitors more challenging. Recently, however, compounds **99**-**101** have emerged as fragment hits from a study utilizing X-ray crystallography for fragment based drug discovery (**Figure 16a**).[119] **99** (PHIP(2) pIC_{50} = 3.9), **100** (PHIP(2) pIC_{50} = 3.7) and **101** (PHIP(2) pIC_{50} = 3.6) together provide three diverse ligand efficient (>0.3) fragments for further optimization in the development of effective PHIP chemical probes, whilst critically demonstrating the potential for atypical bromodomain inhibition.

SP100C

The bromodomain of SP100C contains a Tyr in place of the commonly found Asn and has consequently been more challenging to inhibit effectively. As a result, the targeting of domain-domain interfaces has been proposed instead. Brennan and co-workers have reported two fragment inhibitors (**102** & **103**) of a novel binding site at the plant homeodomain-bromodomain interface. Soaking of SP100C crystals with 412 fragment compounds at 30 mM revealed **102** and **103** as fragment inhibitors of the novel binding site. X-ray crystallography confirmed the binding of the fragments to the identified binding site with no binding to SP100C's bromodomain observed. Although no binding affinities were reported for the two fragments, they do provide insight into a novel approach for atypical bromodomain containing protein target validation, and potential start points for further optimization.

4. Summary & Outlook

Since our last review,[13] the chemical probe research field has become dramatically more advanced and more precisely defined. As a result, the non-BET bromodomain chemical tool portfolio has flourished, with more potent, selective and *in vivo* capable tool molecules being developed. Currently 21/48 typical bromodomain containing proteins have at least 1 bromodomain inhibitor for target validation, with 19/48 possessing ≥3.

The SAR accumulated through the development of bromodomain inhibitors has led to a greater understanding of each individual bromodomain and their key interactions, correlating to an increase in potency of the inhibitors developed over the past 3 and a half years. This is epitomized by CREBBP, for which inhibitors are now being developed with a log unit increase in affinity. Contradictorily, this detailed understanding of bromodomain binding pockets has also led to an increase in the successful development of inactive structurally similar negative controls, crucial in the assigning of phenotypical responses to target inhibition.

Also vital to phenotype assignment is selectivity, which similarly has advanced dramatically since our last review. This is particularly evident with selectivity over the BET bromodomain subfamily, especially important due to the strong phenotype associated with the subfamily. Improved selectivity across the

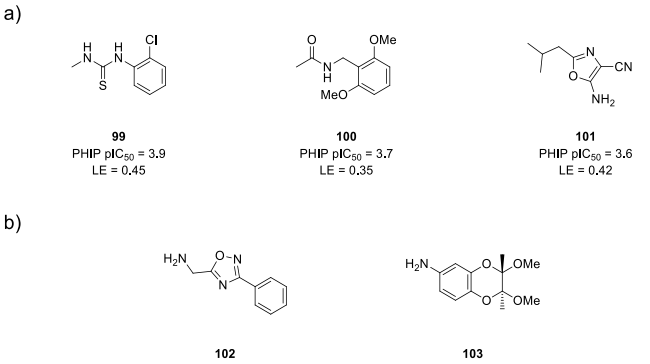

Figure 16. Structures of PHIP fragment hits **99**-**101** and SM100C fragment inhibitors **102** and **103**.

bromodomain family has allowed for more thorough and accurate target validation and will hopefully be maintained for future probe development.

With a culmination of high quality non-BET bromodomain chemical probes, attention has even turned to the possibility of more sophisticated bifunctional tool molecules for target validation. Of particular note has been the development of non-BET PROTACs and their potential for new pharmacology, not possible with bromodomain inhibitors alone.

Despite the growing advances in typical bromodomain inhibition and target validation, the repertoire of atypical bromodomain chemical probes is still in its infancy, with only 2/13 atypical bromodomain containing proteins having any form of reported inhibitor. Consequently, there remains a demand for a greater quantity of atypical bromodomain chemical probes which are also of higher quality. Hopefully moving forward this will be addressed as we begin to unravel the subtleties of atypical bromodomain inhibition. Additionally, advances into more sophisticated tool molecules for each bromodomain, along with continued effort to improve and diversify the inhibitors we develop, will help elucidate the biological tractability of bromodomain containing proteins. With luck this will facilitate sufficient target validation to reduce clinical attrition, and ultimately lead to the development of new therapeutics.

In conclusion, non-BET bromodomain chemical probe development remains an exciting and vibrant area of research, particularly at the interface of academia and industry. Although clear strides have been made, and we are beginning to see this reflected in our understanding of the roles non-BET bromodomains play in modulating disease states, there remains a number of questions unanswered and avenues for improvement that are sure to be filled in the coming years.

Keywords: non-BET bromodomains • chemical probe • target validation • epigenetics • acetylated lysine

References

(1) Egger, G.; Liang, G.; Aparicio, A.; Jones, P. A. *Nature* **2004**, *429*, 457–463.

(2) Allis, C. D.; Jenuwein, T. *Nat. Rev. Genet.* **2016**, *17*, 487–500.

(3) Golbabapour, S.; Abdulla, M. A.; Hajrezaei, M. *Int. J. Mol. Sci.* **2011**, *12*, 8661–8694.

(4) Ali, I.; Conrad, R. J.; Verdin, E.; Ott, M. *Chem. Rev.* **2018**, *118*, 1216–1252.

(5) Dhalluin, C.; Carlson, J. E.; Zeng, L.; He, C.; Aggarwal, A. K.; Zhou, M.-M.; Zhou, M.-M. *Nature* **1999**, *399*, 491–496.

(6) Oprea, T. I.; Bologa, C. G.; Boyer, S.; Curpan, R. F.; Glen, R. C.; Hopkins, A. L.; Lipinski, C. A.; Marshall, G. R.; Martin, Y. C.; Ostopovici-Halip, L.; Rishton, G.; Ursu, O.; Vaz, R. J.; Waller, C.; Waldmann, H.; Sklar, L. A. *Nat. Chem. Biol.* **2009**, *5*, 441–447.

(7) Frye, S. V. *Nat. Chem. Biol.* **2010**, *6*, 159–161.

(8) Arrowsmith, C. H.; Audia, J. E.; Austin, C.; Baell, J.; Bennett, J.; Blagg, J.; Bountra, C.; Brennan, P. E.; Brown, P. J.; Bunnage, M. E.; Buser-Doepner, C.; Campbell, R. M.; Carter, A. J.; Cohen, P.; Copeland, R. A.; Cravatt, B.; Dahlin, J. L.; Dhanak, D.; Edwards, A. M.; Frederiksen, M.; Frye, S. V; Gray, N.; Grimshaw, C. E.; Hepworth, D.; Howe, T.; M Huber, K. V; Jin, J.; Knapp, S.; Kotz, J. D.; Kruger, R. G.; Lowe, D.; Mader, M. M.; Marsden, B.; Mueller-Fahrnow, A.; Müller, S.; O, R. C.; Overington, J. P.; Owen, D. R.; Rosenberg, S. H.; Roth, B.; Ross, R.; Schapira, M.; Schreiber, S. L.; Shoichet, B.; Sundström, M.; Superti-Furga, G.; Taunton, J.; Toledo-Sherman, L.; Walpole, C.; Walters, M. A.; Willson, T. M.; Workman, P.; Young, R. N.; Zuercher, W. J. *Nat. Chem. Biol.* **2015**, *11*, 536–542.

(9) Blagg, J.; Workman, P. *Cancer Cell* **2017**, *32*, 9–25.

(10) Garbaccio, R. M.; Parmee, E. R. *Cell Chem. Biol.* **2016**, *23*, 10–17.

(11) Bunnage, M. E.; Piatnitski Chekler, E. L.; Jones, L. H. *Nat. Chem. Biol.* **2013**, *9*, 195–199.

(12) Moellering, R. E.; Cravatt, B. F. *Chem. Biol.* **2012**, *19*, 11–22.

(13) Theodoulou, N. H.; Tomkinson, N. C. O.; Prinjha, R. K.; Humphreys, P. G. *ChemMedChem* **2016**, *11*, 477–487.

(14) Clegg, M. A.; Tomkinson, N. C.; Prinjha, R. K.; Humphreys, P. G. *Future Med. Chem.* **2017**, *9*, 1579–1582.

(15) Kuo, L. J.; Yang, L.-X. *In Vivo 22*, 305–309.

(16) SGC | NVS-CECR2-1 http://www.thesgc.org/chemical-probes/NVS-1 (accessed Jun 10, 2017).

(17) Crawford, T. D.; Audia, J. E.; Bellon, S.; Burdick, D. J.; Bommi-Reddy, A.; Côté, A.; Cummings, R. T.; Duplessis, M.; Flynn, E. M.; Hewitt, M.; Huang, H.-R.; Jayaram, H.; Jiang, Y.; Joshi, S.; Kiefer, J. R.; Murray, J.; Nasveschuk, C. G.; Neiss, A.; Pardo, E.; Romero, F. A.; Sandy, P.; Sims, R. J.; Tang, Y.; Taylor, A. M.; Tsui, V.; Wang, J.; Wang, S.; Wang, Y.; Xu, Z.; Zawadzke, L.; Zhu, X.; Albrecht, B. K.; Magnuson, S. R.; Cochran, A. G. *ACS Med. Chem. Lett.* **2017**, *8*, 737–741.

(18) Modak, R.; Basha, J.; Bharathy, N.; Maity, K.; Mizar, P.; Bhat, A. V.; Vasudevan, M.; Rao, V. K.; Kok, W. K.; Natesh, N.; Taneja, R.; Kundu, T. K. *ACS Chem. Biol.* **2013**, *8*, 1311–1323.

(19) Malatesta, M.; Steinhauer, C.; Mohammad, F.; Pandey, D. P.; Squatrito, M.; Helin, K. *Cancer Res.* **2013**, *73*, 6323–6333.

(20) Stimson, L.; Rowlands, M. G.; Newbatt, Y. M.; Smith, N. F.; Raynaud, F. I.; Rogers, P.; Bavetsias, V.; Gorsuch, S.; Jarman, M.; Bannister, A.; Kouzarides, T.; McDonald, E.; Workman, P.; Aherne, G. W. *Mol. Cancer Ther.* **2005**, *4*, 1521–1532.

(21) Duclot, F.; Meffre, J.; Jacquet, C.; Gongora, C.; Maurice, T. *Neuroscience* **2010**, *167*, 850–863.

(22) Zhou, M. M.; Gerona-Navarro, G.; Rodriguez-Fernandez, Y.; Casaccia, P. Small Molecule Transcri tion Modulators of Bromodomains. WO15184257, 2015.

(23) Mujtaba, S.; He, Y.; Zeng, L.; Farooq, A.; Carlson, J. E.; Ott, M.; Verdin, E.; Zhou, M.-M. *Mol. Cell* **2002**, *9*, 575–586.

(24) Quy, V. C.; Pantano, S.; Rossetti, G.; Giacca, M.; Carloni, P. *Biology (Basel).* **2012**, *1*, 277–296.

(25) Kiernan, R. E.; Vanhulle, C.; Schiltz, L.; Adam, E.; Xiao, H.; Maudoux, F.; Calomme, C.; Burny, A.; Nakatani, Y.; Jeang, K.; Benkirane, M.; Van Lint, C. *EMBO J.* **1999**, *18*, 6106–6118.

(26) Masumi, A.; Wang, I. M.; Lefebvre, B.; Yang, X. J.; Nakatani, Y.; Ozato, K. *Mol. Cell. Biol.* **1999**, *19*, 1810–1820.

(27) Albrecht, B. K.; Burdick, D. J.; Cote, A.; Duplessis, M.; Nasveschuk, C. G.; Taylor, A. M. Pyridazinone derivatives and their use in the treatment of cancer. WO 2016/112298 A1, 2016.

(28) Albrecht, B. K.; Cote, A.; Crawford, T.; Duplessis, M.; Good, A. C.; Leblanc, Y.; Magnuson, S.; Nasveschuk, C. G.; Pastor, R.; Romero, F. A.; Taylor, A. M. Phthalazine derivatives of formula (1) as PCAF and GCN5 inhibitors for use in the treatment of cancer. WO 2016/036954 A1, 2016.

(29) Albrecht, B. K.; Cote, A.; Crawford, T.; Duplessis, M.; Good, A. C.; Leblanc, Y.; Magnuson, S.; Nasveschuk, C. G.; Pastor, R.; Romero, F. A.; Taylor, A. M. Preparation of 1,2,4-triazine-3,5(2H,4H)-diones as inhibitors of PCAF for treating cancer and other PCAF-mediated disorders. WO 2016/036873 A1, 2016.

(30) Humphreys, P. G.; Bamborough, P.; Chung, C.; Craggs, P. D.; Gordon, L.; Grandi, P.; Hayhow, T. G.; Hussain, J.; Jones, K. L.; Lindon, M.; Michon, A.-M.; Renaux, J. F.; Suckling, C. J.; Tough, D. F.; Prinjha, R. K. *J. Med. Chem.* **2017**, *60*, 695–709.

(31) Moustakim, M.; Clark, P. G. K.; Trulli, L.; Fuentes de Arriba, A. L.; Ehebauer, M. T.; Chaikuad, A.; Murphy, E. J.; Mendez-Johnson, J.; Daniels, D.; Hou, C.-F. D.; Lin, Y.-H.; Walker, J. R.; Hui, R.; Yang, H.; Dorrell, L.; Rogers, C. M.; Monteiro, O. P.; Fedorov, O.; Huber, K. V. M.; Knapp, S.; Heer, J.; Dixon, D. J.; Brennan, P. E. *Angew. Chemie Int. Ed.* **2017**, *56*, 827–831.

(32) Picaud, S.; Leonards, K.; Lambert, J. P.; Dovey, O.; Wells, C.; Fedorov, O.; Monteiro, O.; Fujisawa, T.; Wang, C. Y.; Lingard, H.; Tallant, C.; Nikbin, N.; Guetzoyan, L.; Ingham, R.; Ley, S. V.; Brennan, P.; Muller, S.; Samsonova, A.; Gingras, A. C.; Schwaller, J.; Vassiliou, G.; Knapp, S.; Filippakopoulos, P. *Sci. Adv.* **2016**, *2*, e1600760–e1600760.

(33) Xiao, S.; Liu, L.; Lu, X.; Long, J.; Zhou, X.; Fang, M. *J. Cancer Res. Clin. Oncol.* **2015**, *141*, 1465–1474.

(34) Kim, K.; Punj, V.; Choi, J.; Heo, K.; Kim, J.-M.; Laird, P. W.; An, W. *Epigenetics Chromatin* **2013**, *6*, 34–46.

(35) Dar, A. A.; Nosrati, M.; Bezrookove, V.; de Semir, D.; Majid, S.; Thummala, S.; Sun, V.; Tong, S.; Leong, S. P. L.; Minor, D.; Billings, P. R.; Soroceanu, L.; Debs, R.; Miller, J. R.; Sagebiel, R. W.; Kashani-Sabet, M. *JNCI J. Natl. Cancer Inst.* **2015**, *107*, 1–9.

(36) Buganim, Y.; Goldstein, I.; Lipson, D.; Milyavsky, M.; Polak-Charcon, S.; Mardoukh, C.; Solomon, H.; Kalo, E.; Madar, S.; Brosh, R.; Perelman, M.; Navon, R.; Goldfinger, N.; Barshack, I.; Yakhini, Z.; Rotter, V. *PLoS One* **2010**, *5*, e9657.

(37) Urick, A. K.; Hawk, L. M. L.; Cassel, M. K.; Mishra, N. K.; Liu, S.; Adhikari, N.; Zhang, W.; dos Santos, C. O.; Hall, J. L.; Pomerantz, W. C. K. *ACS Chem. Biol.* **2015**, *10*, 2246–2256.

(38) SGC | Bromodomain of human nucleosome-remodeling factor subunit BPTF http://www.thesgc.org/structures/3uv2 (accessed Jun 10, 2017).

(39) Ianculescu, I.; Wu, D.-Y.; Siegmund, K. D.; Stallcup, M. R. *J. Biol. Chem.* **2012**, *287*, 4000–4013.

(40) Giotopoulos, G.; Chan, W.-I.; Horton, S. J.; Ruau, D.; Gallipoli, P.; Fowler, A.; Crawley, C.; Papaemmanuil, E.; Campbell, P. J.; Göttgens, B.; Van Deursen, J. M.; Cole, P. A.; Huntly, B. J. P. *Oncogene* **2016**, *35*, 279–289.

(41) Iyer, N. G.; Özdag, H.; Caldas, C. *Oncogene* **2004**, *23*, 4225–4231.

(42) Crawford, T. D.; Romero, F. A.; Lai, K. W.; Tsui, V.; Taylor, A. M.; de Leon Boenig, G.; Noland, C. L.; Murray, J.; Ly, J.; Choo, E. F.; Hunsaker, T. L.; Chan, E. W.; Merchant, M.; Kharbanda, S.; Gascoigne, K. E.; Kaufman, S.; Beresini, M. H.; Liao, J.; Liu, W.; Chen, K. X.; Chen, Z.; Conery, A. R.; Côté, A.; Jayaram, H.; Jiang, Y.; Kiefer, J. R.; Kleinheinz, T.; Li, Y.; Maher, J.; Pardo, E.; Poy, F.; Spillane, K. L.; Wang, F.; Wang, J.; Wei, X.; Xu, Z.; Xu, Z.; Yen, I.; Zawadzke, L.; Zhu, X.; Bellon, S.; Cummings, R.; Cochran, A. G.; Albrecht, B. K.; Magnuson, S. *J. Med. Chem.* **2016**, *59*, 10549–10563.

(43) Romero, F. A.; Murray, J.; Lai, K. W.; Tsui, V.; Albrecht, B. K.; An, L.; Beresini, M. H.; de Leon Boenig, G.; Bronner, S. M.; Chan, E. W.; Chen, K. X.; Chen, Z.; Choo, E. F.; Clagg, K.; Clark, K.; Crawford, T. D.; Cyr, P.; de Almeida Nagata, D.; Gascoigne, K. E.; Grogan, J. L.; Hatzivassiliou, G.; Huang, W.; Hunsaker, T. L.; Kaufman, S.; Koenig, S. G.; Li, R.; Li, Y.; Liang, X.; Liao, J.; Liu, W.; Ly, J.; Maher, J.; Masui, C.; Merchant, M.; Ran, Y.; Taylor, A. M.; Wai, J.; Wang, F.; Wei, X.; Yu, D.; Zhu, B.-Y.; Zhu, X.; Magnuson, S. *J. Med. Chem.* **2017**, *60*, 9162–9183.

(44) Sakaguchi, S.; Yamaguchi, T.; Nomura, T.; Ono, M. *Cell* **2008**, *133*, 775–787.

(45) Bronner, S. M.; Murray, J.; Romero, F. A.; Lai, K. W.; Tsui, V.; Cyr, P.; Beresini, M. H.; de leon Boenig, G.; Chen, Z.; Choo, E. F.; Clark, K. R.; Crawford, T. D.; Jayaram, H.; Kaufman, S.; Li, R.; Li, Y.; Liao, J.; Liang, X.; Liu, W.; Ly, J.; Maher, J.; Wai, J.; Wang, F.; Zheng, A.; Zhu, X.; Magnuson, S. *J. Med. Chem.* **2017**, *60*, 10151–10171.

(46) Denny, R. A.; Flick, A. C.; Coe, J.; Langille, J.; Basak, A.; Liu, S.; Stock, I.; Sahasrabudhe, P.; Bonin, P.; Hay, D. A.; Brennan, P. E.; Pletcher, M.; Jones, L. H.; Chekler, E. L. P. *J. Med. Chem.* **2017**, *60*, 5349–5363.

(47) Hett, E. C.; Piatnitski Chekler, E. L.; Basak, A.; Bonin, P. D.; Denny, R. A.; Flick, A. C.; Geoghegan, K. F.; Liu, S.; Pletcher, M. T.; Sahasrabudhe, P.; Salter, S. C.; Stock, I. A.; Taylor, A. P.; Jones, L. H. *Medchemcomm* **2015**, *6*, 1018–1023.

(48) Xiang, Q.; Wang, C.; Zhang, Y.; Xue, X.; Song, M.; Zhang, C.; Li, C.; Wu, C.; Li, K.; Hui, X.; Zhou, Y.; Smaill, J. B.; Patterson, A. V.; Wu, D.; Ding, K.; Xu, Y. *Eur. J. Med. Chem.* **2018**, *147*, 238–252.

(49) Lucas, X.; Wohlwend, D.; Hügle, M.; Schmidtkunz, K.; Gerhardt, S.; Schüle, R.; Jung, M.; Einsle, O.; Günther, S. *Angew. Chemie Int. Ed.* **2013**, *52*, 14055–14059.

(50) Picaud, S.; Fedorov, O.; Thanasopoulou, A.; Leonards, K.; Jones, K.; Meier, J.; Olzscha, H.; Monteiro, O.; Martin, S.; Philpott, M.; Tumber, A.; Filippakopoulos, P.; Yapp, C.; Wells, C.; Che, K. H.; Bannister, A.; Robson, S.; Kumar, U.; Parr, N.; Lee, K.; Lugo, D.; Jeffrey, P.; Taylor, S.; Vecellio, M. L.; Bountra, C.; Brennan, P. E.; O'Mahony, A.; Velichko, S.; Müller, S.; Hay, D.; Daniels, D. L.; Urh, M.; La Thangue, N. B.; Kouzarides, T.; Prinjha, R.; Schwaller, J.; Knapp, S. *Cancer Res.* **2015**, *75*, 5106–5119.

(51) Popp, T. A.; Tallant, C.; Rogers, C.; Fedorov, O.; Brennan, P. E.; Müller, S.; Knapp, S.; Bracher, F. *J. Med. Chem.* **2016**, *59*, 8889–8912.

(52) Taylor, A. M.; Côté, A.; Hewitt, M. C.; Pastor, R.; Leblanc, Y.; Nasveschuk, C. G.; Romero, F. A.; Crawford, T. D.; Cantone, N.; Jayaram, H.; Setser, J.; Murray, J.; Beresini, M. H.; de Leon Boenig, G.; Chen, Z.; Conery, A. R.; Cummings, R. T.; Dakin, L. A.; Flynn, E. M.; Huang, O. W.; Kaufman, S.; Keller, P. J.; Kiefer, J. R.; Lai, T.; Li, Y.; Liao, J.; Liu, W.; Lu, H.; Pardo, E.; Tsui, V.; Wang, J.; Wang, Y.; Xu, Z.; Yan, F.; Yu, D.; Zawadzke, L.; Zhu, X.; Zhu, X.; Sims, R. J.; Cochran, A. G.; Bellon, S.; Audia, J. E.; Magnuson, S.; Albrecht, B. K. *ACS Med. Chem. Lett.* **2016**, *7*, 531–536.

(53) Romero, Anthony, F.; Magnuson, S.; Pastor, R.; Tsui, V. H.-W.; Murray, J.; Crawford, T.; Albrecht, B. K.; Cote, A.; Taylor, A. M.; Lai, K. W.; Chen, K. X. Minesoft Patent Order. WO 2016/086200 A1, 2016.

(54) Cyr, P.; Bronner, S.; Romero, F. A.; Magnuson, S.; Tsui, V. H.-W.; Muray, J. M.; Wai, J.; Lai, K. W.; Wang, F.; Chen, K. X. Trace Order. WO 2017/205538 A1, 2017.

(55) Romero, A. F.; Magnuson, S. R.; Pastor, R.; Tsui, V. H.-W.; Murray, J.; Crawford, T.; Burdick, D. J.; Albrecht, B. K.; Coff, A.; Taylor, A. M.; Nasveshuk, C. G.; Leblanc, Y.; Hewitt, M. C.; Lai, K. W.; Chen, K. THERAPEUTIC COMPOUNDS AND USES THEREOF. WO 2016/055028 A1, 2016.

(56) Pegg, N. A.; Taddei, D. M. A.; Shannon, J.; Paoletta, S.; Qin, T.; Harbottle, G. WO 2018/073587 A1. WO 2018/073587 A1, 2018.

(57) Pegg, N. A.; Onions, S. T.; Taddei, D. M. A.; Shannon, J.; Paoletta, S.; Brown, R. J.; Smyth, D.; Harbottle, G. Trace Order. WO 2018/073586 A1, 2018.

(58) Bennet, M. J.; Betancort, J. M.; Boloor, A.; Kanouni, T.; Stafford, J. A.; Veal, J. M.; Wallace, M. B. Trace Order. US 2017/0298040 A1, 2017.

(59) Sakamoto, K. M.; Smith, M.; Chae, H.-D.; Mitton, B.; Cox, N. R. WO 2017/156489. WO 2017/156489, 2017.

(60) Blázquez Nevado, C.; Caflisch, A.; Unzue Lopez, A.; Xu, M.; Dong, J.; Spiliotopoulos, D.; Frugier, E.; Dolbois, A. COMPOUNDS, IN PARTICULAR FOR USE IN THE TREATMENT OF A DISEASE OR CONDITION FOR WHICH A BROMODOMAIN INHIBITOR IS INDICATED. WO 2016/001452 A1, 2016.

(61) Brown, T.; Swansbury, J.; Taj, M. M. *Leuk. Lymphoma* **2012**, *53*, 338–341.

(62) Carlson, S.; Glass, K. C. *J. Cell. Physiol.* **2014**, *229*, 1571–1574.

(63) Demont, E. H.; Bamborough, P.; Chung, C.; Craggs, P. D.; Fallon, D.; Gordon, L. J.; Grandi, P.; Hobbs, C. I.; Hussain, J.; Jones, E. J.; Le Gall, A.; Michon, A.-M.; Mitchell, D. J.; Prinjha, R. K.; Roberts, A. D.; Sheppard, R. J.; Watson, R. J. *ACS Med. Chem. Lett.* **2014**, *5*, 1190–1195.

(64) Bamborough, P.; Barnett, H. A.; Becher, I.; Bird, M. J.; Chung, C.; Craggs, P. D.; Demont, E. H.; Diallo, H.; Fallon, D. J.; Gordon, L. J.; Grandi, P.; Hobbs, C. I.; Hooper-Greenhill, E.; Jones, E. J.; Law, R. P.; Le Gall, A.; Lugo, D.; Michon, A.-M.; Mitchell, D. J.; Prinjha, R. K.; Sheppard, R. J.; Watson, A. J. B.; Watson, R. J. *ACS Med. Chem. Lett.* **2016**, *7*, 552–557.

(65) Bamborough, P.; Chung, C.-W.; Gall, A.; Sheppard, R. J. 1,3-DIMETHYLBENZIMIDAZOLONE DERIVATIVE AS AN INHIBITOR OF THE BRPFI BROMODOMAIN. WO 2016/062737 A1, 2016.

(66) Bouché, L.; Christ, C. D.; Siegel, S.; Fernández-Montalván, A. E.; Holton, S. J.; Fedorov, O.; ter Laak, A.; Sugawara, T.; Stöckigt, D.; Tallant, C.; Bennett, J.; Monteiro, O.; Díaz-Sáez, L.; Siejka, P.; Meier, J.; Pütter, V.; Weiske, J.; Müller, S.; Huber, K. V. M.; Hartung, I. V.; Haendler, B. *J. Med. Chem.* **2017**, *60*, 4002–4022.

(67) Bouché, L. A.; Siegel, S.; Haendler Bernard; Christ, C.; Ter Laak, A.; Fernandez-Montalvan, A.; Stöckigt, D.; Holton, S. IH-BENZO[DEJISOQUINOLINE- 1,3(211)-DIONES. WO 2017/162661 A1, 2017.

(68) Zhu, J.; Zhou, C.; Caflisch, A. *Eur. J. Med. Chem.* **2018**, *155*, 337–352.

(69) Fish, P. V.; Igoe, N.; Bayle, E. D. QUINOLONES AS INHIBITORS OF CLASS IV BROMODOMAIN PROTEINS. WO 2016/034512, 2016.

(70) Hohmann, A. F.; Vakoc, C. R. *Trends Genet.* **2014**, *30*, 356–363.

(71) Liu, Y.; Zhao, R.; Wang, H.; Luo, Y.; Wang, X.; Niu, W.; Zhou, Y.; Wen, Q.; Fan, S.; Li, X.; Xiong, W.; Ma, J.; Li, X.; Tan, M.; Li, G.; Zhou, M. *Cell Death Dis.* **2016**, *7*, e2156.

(72) Yu, X.; Li, Z.; Shen, J. *Am. J. Transl. Res.* **2016**, *8*, 742–748.

(73) Drost, J.; Mantovani, F.; Tocco, F.; Elkon, R.; Comel, A.; Holstege, H.; Kerkhoven, R.; Jonkers, J.; Voorhoeve, P. M.; Agami, R.; Del Sal, G. *Nat. Cell Biol.* **2010**, *12*, 380–389.

(74) Cleary, S. P.; Jeck, W. R.; Zhao, X.; Chen, K.; Selitsky, S. R.; Savich,

G. L.; Tan, T.-X.; Wu, M. C.; Getz, G.; Lawrence, M. S.; Parker, J. S.; Li, J.; Powers, S.; Kim, H.; Fischer, S.; Guindi, M.; Ghanekar, A.; Chiang, D. Y. *Hepatology* **2013**, *58*, 1693–1702.

(75) Martin, L. J.; Koegl, M.; Bader, G.; Cockcroft, X.-L.; Fedorov, O.; Fiegen, D.; Gerstberger, T.; Hofmann, M. H.; Hohmann, A. F.; Kessler, D.; Knapp, S.; Knesl, P.; Kornigg, S.; Müller, S.; Nar, H.; Rogers, C.; Rumpel, K.; Schaaf, O.; Steurer, S.; Tallant, C.; Vakoc, C. R.; Zeeb, M.; Zoephel, A.; Pearson, M.; Boehmelt, G.; McConnell, D. *J. Med. Chem.* **2016**, *59*, 4462–4475.

(76) BI-9564 https://opnme.com/molecules/brd9-bi9564 (accessed Aug 24, 2018).

(77) SGC | TP-472 http://www.thesgc.org/chemical-probes/TP-472 (accessed Jun 11, 2017).

(78) Crawford, T. D.; Tsui, V.; Flynn, E. M.; Wang, S.; Taylor, A. M.; Côé, A.; Audia, J. E.; Beresini, M. H.; Burdick, D. J.; Cummings, R.; Dakin, L. A.; Duplessis, M.; Good, A. C.; Hewitt, M. C.; Huang, H.-R.; Jayaram, H.; Kiefer, J. R.; Jiang, Y.; Murray, J.; Nasveschuk, C. G.; Pardo, E.; Poy, F.; Romero, F. A.; Tang, Y.; Wang, J.; Xu, Z.; Zawadzke, L. E.; Zhu, X.; Albrecht, B. K.; Magnuson, S. R.; Bellon, S.; Cochran, A. G. *J. Med. Chem.* **2016**, *59*, 5391–5402.

(79) Crawford, T. D.; Vartanian, S.; Côté, A.; Bellon, S.; Duplessis, M.; Flynn, E. M.; Hewitt, M.; Huang, H.-R.; Kiefer, J. R.; Murray, J.; Nasveschuk, C. G.; Pardo, E.; Romero, F. A.; Sandy, P.; Tang, Y.; Taylor, A. M.; Tsui, V.; Wang, J.; Wang, S.; Zawadzke, L.; Albrecht, B. K.; Magnuson, S. R.; Cochran, A. G.; Stokoe, D. *Bioorg. Med. Chem. Lett.* **2017**, *27*, 3534–3541.

(80) Raha, D.; Wilson, T. R.; Peng, J.; Peterson, D.; Yue, P.; Evangelista, M.; Wilson, C.; Merchant, M.; Settleman, J. *Cancer Res.* **2014**, *74*, 3579–3590.

(81) Wang, N.; Li, F.; Bao, H.; Li, J.; Wu, J.; Ruan, K. *ChemBioChem* **2016**, *17*, 1456–1463.

(82) Albrecht, B. K.; Cote, A.; Crawford, T.; Fauber, B.; Huang, H.-R.; Lore, J. M.; Magnuson, S.; Nasveschuk, C. G.; Salmeron, A.; Sims, R. J.; Taylor, A. M. Treating TH2-Mediated diseases by inhibition of bromodomains. US 2016/0024504 A1, 2016.

(83) Martin, L.; Steurer, S.; Cockcroft, X.-L. NEW PYRIDINONES AND ISOQUINOLINONES AS INHIBITORS OF THE BROMODOMAIN BRD9. WO 2016/139361 A1, 2016.

(84) Remillard, D.; Buckley, D. L.; Paulk, J.; Brien, G. L.; Sonnett, M.; Seo, H.-S.; Dastjerdi, S.; Wühr, M.; Dhe-Paganon, S.; Armstrong, S. A.; Bradner, J. E. *Angew. Chemie Int. Ed.* **2017**, *56*, 5738–5743.

(85) Caron, C.; Lestrat, C.; Marsal, S.; Escoffier, E.; Curtet, S.; Virolle, V.; Barbry, P.; Debernardi, A.; Brambilla, C.; Brambilla, E.; Rousseaux, S.; Khochbin, S. *Oncogene* **2010**, *29*, 5171–5181.

(86) Chen, X.; Cheung, S. T.; So, S.; Fan, S. T.; Barry, C.; Higgins, J.; Lai, K.-M.; Ji, J.; Dudoit, S.; Ng, I. O. L.; Van De Rijn, M.; Botstein, D.; Brown, P. O. *Mol. Biol. Cell* **2002**, *13*, 1929–1939.

(87) Raeder, M. B.; Birkeland, E.; Trovik, J.; Krakstad, C.; Shehata, S.; Schumacher, S.; Zack, T. I.; Krohn, A.; Werner, H. M.; Moody, S. E.; Wik, E.; Stefansson, I. M.; Holst, F.; Oyan, A. M.; Tamayo, P.; Mesirov, J. P.; Kalland, K. H.; Akslen, L. A.; Simon, R.; Beroukhim, R.; Salvesen, H. B. *PLoS One* **2013**, *8*, e54873.

(88) Ciro, M.; Prosperini, E.; Quarto, M.; Grazini, U.; Walfridsson, J.; McBlane, F.; Nucifero, P.; Pacchiana, G.; Capra, M.; Christensen, J.; Helin, K. *Cancer Res.* **2009**, *69*, 8491–8498.

(89) Bamborough, P.; Chung, C.; Furze, R. C.; Grandi, P.; Michon, A.-M.; Sheppard, R. J.; Barnett, H.; Diallo, H.; Dixon, D. P.; Douault, C.; Jones, E. J.; Karamshi, B.; Mitchell, D. J.; Prinjha, R. K.; Rau, C.; Watson, R. J.; Werner, T.; Demont, E. H. *J. Med. Chem.* **2015**, *58*, 6151–6178.

(90) SGC | GSK8814 http://www.thesgc.org/chemical-probes/GSK8814 (accessed Jun 11, 2017).

(91) Bamborough, P.; Chung, C.; Furze, R. C.; Grandi, P.; Michon, A.-M.; Watson, R. J.; Mitchell, D. J.; Barnett, H.; Prinjha, R. K.; Rau, C.; Sheppard, R. J.; Werner, T.; Demont, E. H. *J. Med. Chem.* **2018**, *61*, 8321–8336.

(92) Fernández-Montalván, A. E.; Berger, M.; Kuropka, B.; Koo, S. J.; Badock, V.; Weiske, J.; Puetter, V.; Holton, S. J.; Stöckigt, D.; ter Laak, A.; Centrella, P. A.; Clark, M. A.; Dumelin, C. E.; Sigel, E. A.; Soutter, H. H.; Troast, D. M.; Zhang, Y.; Cuozzo, J. W.; Keefe, A. D.; Roche, D.; Rodeschini, V.; Chaikuad, A.; Díaz-Sáez, L.; Bennett, J. M.; Fedorov, O.; Huber, K. V. M.; Hübner, J.; Weinmann, H.; Hartung, I. V.; Gorjánácz, M. *ACS Chem. Biol.* **2017**, *12*, 2730–2736.

(93) Miller, D. C.; Martin, M. P.; Adhikari, S.; Brennan, A.; Endicott, J. A.; Golding, B. T.; Hardcastle, I. R.; Heptinstall, A.; Hobson, S.; Jennings, C.; Molyneux, L.; Ng, Y.; Wedge, S. R.; Noble, M. E. M.; Cano, C. *Org. Biomol. Chem.* **2018**, *16*, 1843–1850.

(94) Chambon, M.; Orsetti, B.; Berthe, M.-L.; Bascoul-Mollevi, C.; Rodriguez, C.; Duong, V.; Gleizes, M.; Thénot, S.; Bibeau, F.; Theillet, C.; Cavaillès, V. *Am. J. Pathol.* **2011**, *178*, 1461–1469.

(95) Li, H.; Sun, L.; Tang, Z.; Fu, L.; Xu, Y.; Li, Z.; Luo, W.; Qiu, X.; Wang, E. *PLoS One* **2012**, *7* (5), e37657.

(96) Cui, Z.; Cao, W.; Li, J.; Song, X.; Mao, L.; Chen, W. *PLoS One* **2013**, *8*, e63887.

(97) Zhan, Y.; Kost-Alimova, M.; Shi, X.; Leo, E.; Bardenhagen, J. P.; Shepard, H. E.; Appikonda, S.; Vangamudi, B.; Zhao, S.; Tieu, T. N.; Jiang, S.; Heffernan, T. P.; Marszalek, J. R.; Toniatti, C.; Draetta, G.; Tyler, J.; Barton, M.; Jones, P.; Palmer, W. S.; Geck Do, M. K.; Andersen, J. N. *Epigenetics Chromatin* **2015**, *8*, 1–19.

(98) Gechijian, L. N.; Buckley, D. L.; Lawlor, M. A.; Reyes, J. M.; Paulk, J.; Ott, C. J.; Winter, G. E.; Erb, M. A.; Scott, T. G.; Xu, M.; Seo, H.-S.; Dhe-Paganon, S.; Kwiatkowski, N. P.; Perry, J. A.; Qi, J.; Gray, N. S.; Bradner, J. E. *Nat. Chem. Biol.* **2018**, *14*, 405.

(99) Gu, L.; Frommel, S. C.; Oakes, C. C.; Simon, R.; Grupp, K.; Gerig, C. Y.; Bär, D.; Robinson, M. D.; Baer, C.; Weiss, M.; Gu, Z.; Schapira, M.; Kuner, R.; Sültmann, H.; Provenzano, M.; Yaspo, M.-L.; Brors, B.; Korbel, J.; Schlomm, T.; Sauter, G.; Eils, R.; Plass, C.; Santoro, R. *Nat. Genet.* **2015**, *47*, 22–30.

(100) Spiliotopoulos, D.; Wamhoff, E.-C.; Lolli, G.; Rademacher, C.; Caflisch, A. *Eur. J. Med. Chem.* **2017**, *139*, 564–572.

(101) Centeno, F.; Ramírez-Salazar, E.; García-Villa, E.; Gariglio, P.; Garrido, E. *Intervirology* **2008**, *51*, 137–143.

(102) Tavassoli, P.; Wafa, L. A.; Cheng, H.; Zoubeidi, A.; Fazli, L.; Gleave, M.; Snoek, R.; Rennie, P. S. *Mol. Endocrinol.* **2010**, *24*, 696–708.

(103) Oh, H. R.; An, C. H.; Yoo, N. J.; Lee, S. H. *Pathol. Oncol. Res.* **2017**, *23*, 125–130.

(104) O 'rawe, J. A.; Wu, Y.; Dörfel, M. J.; Rope, A. F.; Au, P. Y. B.; Parboosingh, J. S.; Moon, S.; Kousi, M.; Kosma, K.; Smith, C. S.; Tzetis, M.; Schuette, J. L.; Jiménez-Barró, L. T.; Monaghan, K. G.; Wang, K.; Davis, E. E.; Katsanis, N.; Kalscheuer, V. M.; Wang, E. H.; Metcalfe, K.; Kleefstra, T.; Innes, A. M.; Kitsiou-Tzeli, S.; Rosello, M.; Keegan, C. E.; Lyon, G. J. *Am. J. Hum. Genet.* **2015**, *97*, 922–932.

(105) Makino, S.; Kaji, R.; Ando, S.; Tomizawa, M.; Yasuno, K.; Goto, S.; Matsumoto, S.; Tabuena, M. D.; Maranon, E.; Dantes, M.; Lee, L. V; Ogasawara, K.; Tooyama, I.; Akatsu, H.; Nishimura, M.; Tamiya, G. *Am. J. Hum. Genet.* **2007**, *80*, 393–406.

(106) Sdelci, S.; Lardeau, C.-H.; Tallant, C.; Klepsch, F.; Klaiber, B.; Bennett, J.; Rathert, P.; Schuster, M.; Penz, T.; Fedorov, O.; Superti-Furga, G.; Bock, C.; Zuber, J.; Huber, K. V. M.; Knapp, S.; Müller, S.; Kubicek, S. *Nat. Chem. Biol.* **2016**, *12*, 504–510.

(107) Sdelci, S.; Kubicek, S. Trace Order. WO 2017/140728 A1, 2017.

(108) Adler, M.; Burdick, D. J.; Crawford, T.; Duplessis, M.; Magnuson, S.; Nasveschuk, C. G.; Romero, F. A.; Tang, Y.; Tsui, V. H. and Wang,

S. Therapeutic compounds and uses thereof. WO 2016/123391 A1, 2016.

(109) Wang, S.; Tsui, V.; Crawford, T. D.; Audia, J. E.; Burdick, D. J.; Beresini, M. H.; Côté, A.; Cummings, R.; Duplessis, M.; Flynn, E. M.; Hewitt, M. C.; Huang, H.-R.; Jayaram, H.; Jiang, Y.; Joshi, S.; Murray, J.; Nasveschuk, C. G.; Pardo, E.; Poy, F.; Romero, F. A.; Tang, Y.; Taylor, A. M.; Wang, J.; Xu, Z.; Zawadzke, L. E.; Zhu, X.; Albrecht, B. K.; Magnuson, S. R.; Bellon, S.; Cochran, A. G. *J. Med. Chem.* **2018**, acs.jmedchem.8b01225.

(110) Suh, J. L.; Watts, B.; Stuckey, J. I.; Norris-Drouin, J. L.; Cholensky, S. H.; Dickson, B. M.; An, Y.; Mathea, S.; Salah, E.; Knapp, S.; Khan, A.; Adams, A. T.; Strahl, B. D.; Sagum, C. A.; Bedford, M. T.; James, L. I.; Kireev, D. B.; Frye, S. V. *Biochemistry* **2018**, *57*, 2140–2149.

(111) Medina, P. P.; Carretero, J.; Fraga, M. F.; Esteller, M.; Sidransky, D.; Sanchez-Cespedes, M. *Genes, Chromosom. Cancer* **2004**, *41*, 170–177.

(112) Singh, M.; Popowicz, G. M.; Krajewski, M.; Holak, T. A. *ChemBioChem* **2007**, *8*, 1308–1316.

(113) Sutherell, C. L.; Tallant, C.; Monteiro, O. P.; Yapp, C.; Fuchs, J. E.; Fedorov, O.; Siejka, P.; Müller, S.; Knapp, S.; Brenton, J. D.; Brennan, P. E.; Ley, S. V. *J. Med. Chem.* **2016**, *59*, 5095–5101.

(114) Albrecht, B. K.; Cote, A.; Crawford, T.; Duplessis, M.; Good, A. C.; Leblanc, Y.; Magnuson, S. R.; Nasveschuk, C. G.; Romero, A. F.; Tang, Y.; Taylor, A. M. Therapeutic pyridazine compounds and uses thereof. WO 2016/138114 A1, 2016.

(115) Lu, T.; Hu, J.; Lu, W.; Han, J.; Ding, H.; Jiang, H.; Zhang, Y.; Yue, L.; Chen, S.; Jiang, H.; Chen, K.; Chai, H.; Luo, C. *Acta Pharmacol. Sin.* **2018**, *39*, 1544–1552.

(116) De Semir, D.; Nosrati, M.; Bezrookove, V.; A. Dar, A.; Federman, S.; Bienvenu, G.; Venna, S.; Rangel, J.; Climent, J.; Tamgüney, T. M. M.; Thummala, S.; Tong, S.; Leong, S. P. L.; Haqq, C.; Billings, P.; Miller, J. R.; Sagebiel, R. W.; Debs, R.; Kashani-Sabet, M. *Proc. Natl. Acad. Sci. U. S. A.* **2012**, *109*, 7067–7072.

(117) Haqq, C.; Nosrati, M.; Sudilovsky, D.; Crothers, J.; Khodabakhsh, D.; Pulliam, B. L.; Federman, S.; Miller, J. R.; Allen, R. E.; Singer, M. I.; Leong, S. P. L.; Ljung, B.-M.; Sagebiel, R. W.; Kashani-Sabet, M. *Proc. Natl. Acad. Sci. U. S. A.* **2005**, *102*, 6092–6097.

(118) de Semir, D.; Bezrookove, V.; Nosrati, M.; Dar, A. A.; Wu, C.; Shen, J.; Rieken, C.; Venkatasubramanian, M.; Miller, J. R.; Desprez, P.-Y.; McAllister, S.; Soroceanu, L.; Debs, R. J.; Salomonis, N.; Schadendorf, D.; Cleaver, J. E.; Kashani-Sabet, M. *Proc. Natl. Acad. Sci. U. S. A.* **2018**, *115*, E5766–E5775.

(119) Cox, O. B.; Krojer, T.; Collins, P.; Monteiro, O.; Talon, R.; Bradley, A.; Fedorov, O.; Amin, J.; Marsden, B. D.; Spencer, J.; von Delft, F.; Brennan, P. E. *Chem. Sci.* **2016**, *7*, 2322–2330.

Entry for the Table of Contents

REVIEW

This review summarizes the advances made in the field of non-BET chemical probe development over the past 3 years. All non-BET chemical probes disclosed within this time frame have been included, highlighting their applicability for target validation and the roles they play in expanding the non-BET chemical tool landscape.

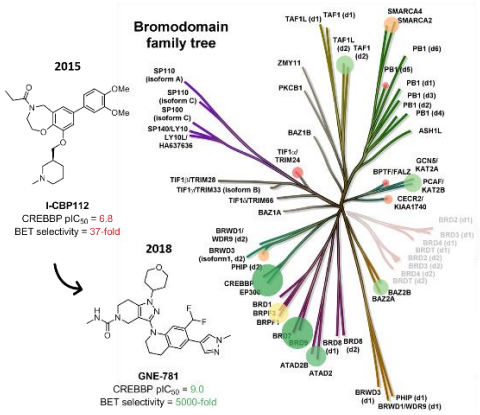

*Michael A. Clegg, Nicholas C. O. Tomkinson, Rab K. Prinjha and Philip G. Humphreys**

Page No. – Page No.

Advancements in the Development of non-BET Bromodomain Chemical Probes